

Tutorial: Magnonics

Burkard Hillebrands

Fachbereich Physik and Landesforschungszentrum OPTIMAS
Technische Universität Kaiserslautern, Germany



Tutorial: Magnonics

Burkard Hillebrands

Fachbereich Physik and Landesforschungszentrum
Technische Universität Kaiserslautern

Happy Birthday, Jairo



Post CMOS?

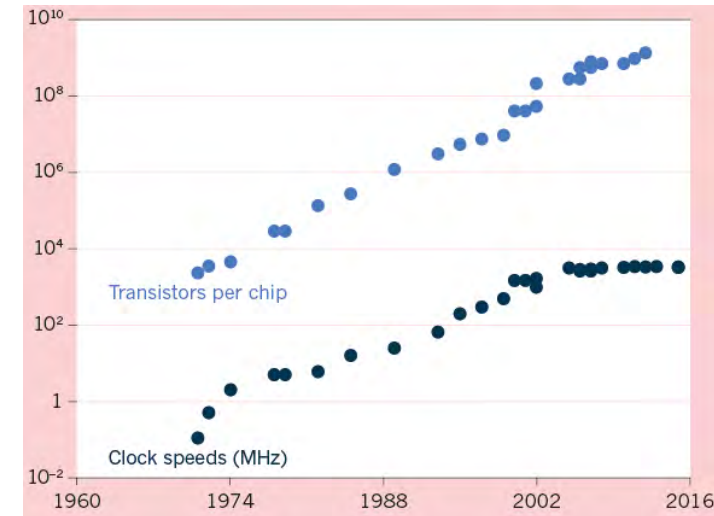
CMOS is coming to the end of Moore's law

- Waste energy production
- End of scaling

Beyond current CMOS:

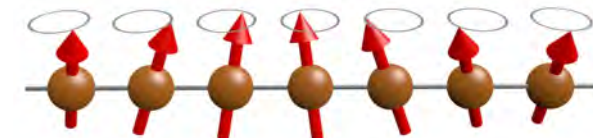
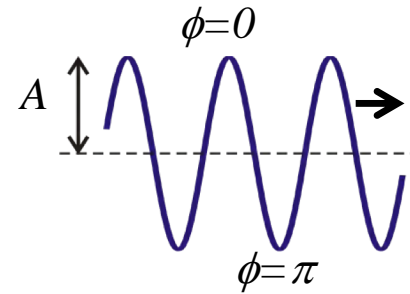
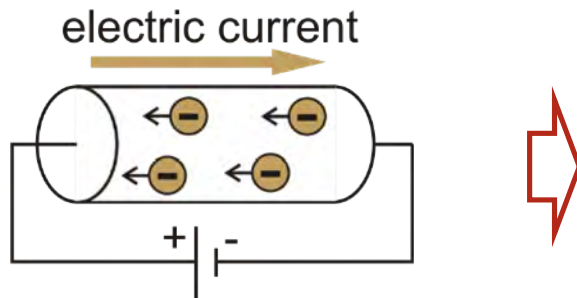
- Faster computing, less energy consumption
- Same technology for logic and data
- Logic circuits with reduced footprint and/or 3D

Novel paradigm: wave computing



M. Mitchell, Nature 530, 144 (2016)

Proposal: use waves /wave packets instead of particles (electrons) for bit representation

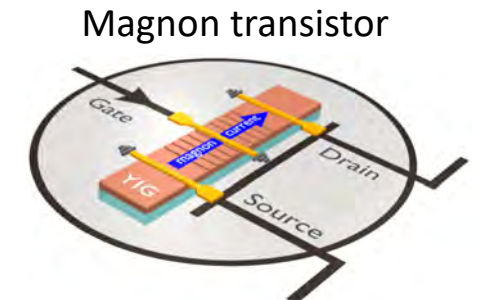
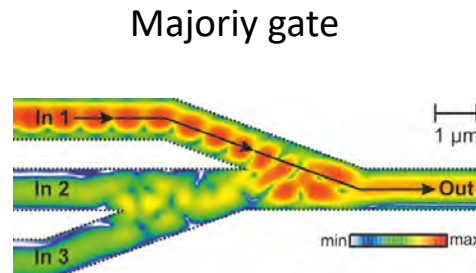
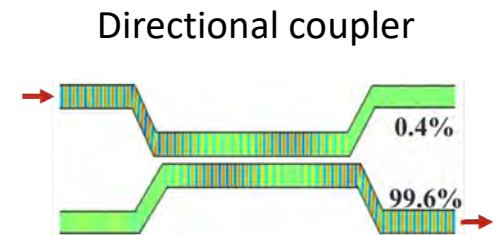
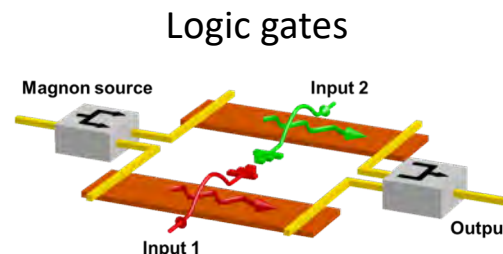


Magnon computing

Why spin waves?

- wavelength down to nanometer, frequency up to several THz
- interference effects easily accessible
- efficient nonlinear effects
- room temperature
- no Joule heat, “insulatronics”
- wave-based computing: smaller footprint, all-wave logic
- good converters to CMOS
→ “magnon spintronics”

Achievements

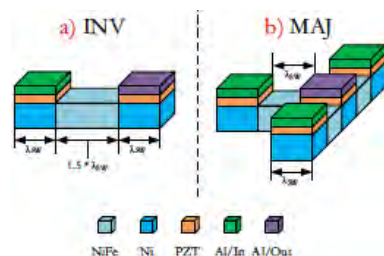


Andrii Chumak, Kaiserslautern

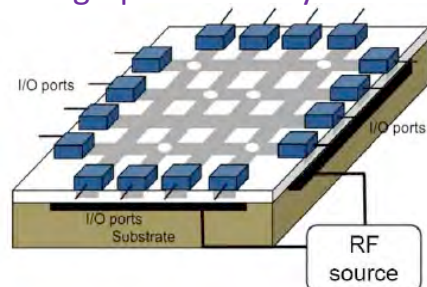
Spin-wave device architectures

L. Amarú, P.-E. Gaillardon,
G. De Micheli
(EPFL, Switzerland)

Majority based synthesis for
nanotechnologies

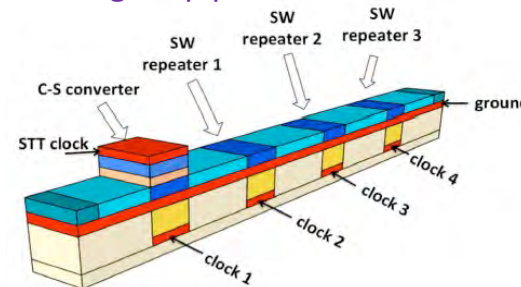


A. Khitun
(Univ. of California Riverside, USA)
Majority gate,
holographic memory



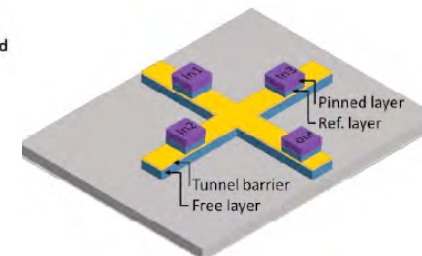
S. Dutta, A. Naeemi
(Georgia Institute of Technology, USA)

Non-volatile clocked spin wave
nanomagnet pipelines

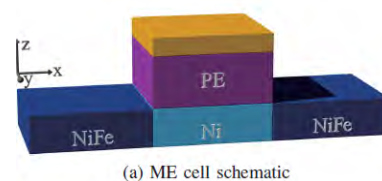


D. E. Nikonov, I. A. Young
(Intel Corp. Hillsboro, Oregon,
USA)

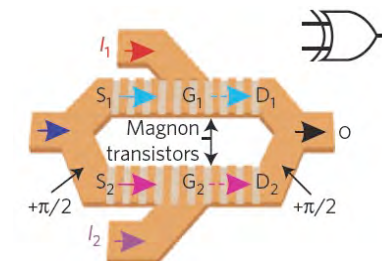
Benchmarking,
clocked spin-wave circuits



F. Ciubotaru, C. Adelmann
(Imec, Leuven, Belgium)
Magnetoacoustic nanoresonators



A. Chumak
(TU Kaiserslautern, Germany)
Magnon transistor,
integrated magnonic circuits



Benchmarking

Hybrid CMOS-Spin Wave Device Circuits Compared to 10nm CMOS

TABLE IV. SUMMARY OF BENCHMARKING RESULTS

| Name | Area (μm^2) | | | | Energy (fJ) | Delay (ns) | | Power (μW) | | ADPP* | | |
|----------|--------------------|---------|-----------|-----------|-------------|------------|-----------|-------------------|-----------|-------------------|-------------------|-----------|
| | SWD core | CMOS SA | SWD Total | 10nm Ref. | | SWD | 10nm Ref. | SWD | 10nm Ref. | SWD | 10nm Ref. | Impr. (x) |
| BKA264 | 36.48 | 3.12 | 39.60 | 118.55 | 175.50 | 5.07 | 0.21 | 34.62 | 133.92 | $6.95 \cdot 10^3$ | $3.33 \cdot 10^3$ | 0.48 |
| HCA464 | 82.71 | 3.17 | 85.88 | 262.63 | 178.20 | 8.01 | 0.29 | 22.25 | 594.28 | $1.53 \cdot 10^4$ | $4.53 \cdot 10^4$ | 2.96 |
| CSA464 | 78.42 | 3.17 | 81.59 | 240.26 | 178.20 | 7.59 | 1.78 | 23.48 | 663.17 | $1.45 \cdot 10^4$ | $2.84 \cdot 10^5$ | 19.51 |
| DTM32 | 326.31 | 3.07 | 329.38 | 1183.64 | 172.80 | 14.73 | 0.52 | 11.73 | 3667.50 | $5.69 \cdot 10^4$ | $2.26 \cdot 10^6$ | 39.66 |
| WTM32 | 264.96 | 3.07 | 268.04 | 1163.37 | 172.80 | 20.61 | 0.58 | 8.38 | 3571.90 | $4.63 \cdot 10^4$ | $2.41 \cdot 10^6$ | 52.04 |
| DTM64 | 1192.69 | 6.14 | 1198.83 | 3459.32 | 345.60 | 18.09 | 0.63 | 19.10 | 12793.10 | $4.14 \cdot 10^5$ | $2.79 \cdot 10^7$ | 67.29 |
| GFMUL | 44.09 | 0.82 | 44.91 | 162.98 | 45.90 | 7.17 | 0.16 | 6.40 | 433.92 | $2.06 \cdot 10^3$ | $1.13 \cdot 10^4$ | 5.49 |
| MAC32 | 295.25 | 3.12 | 298.37 | 1372.83 | 175.50 | 24.39 | 0.66 | 7.20 | 3872.10 | $5.24 \cdot 10^4$ | $3.51 \cdot 10^6$ | 67.00 |
| DIV32 | 899.04 | 6.14 | 905.18 | 3347.73 | 345.60 | 117.21 | 14.00 | 2.95 | 5346.10 | $3.13 \cdot 10^5$ | $2.51 \cdot 10^8$ | 800.94 |
| CRC32 | 27.61 | 1.54 | 29.14 | 95.88 | 86.40 | 5.07 | 0.22 | 17.04 | 304.30 | $2.52 \cdot 10^3$ | $6.42 \cdot 10^3$ | 2.55 |
| Averages | 324.76 | 3.34 | 328.09 | 1140.72 | 187.65 | 22.79 | 1.91 | 15.31 | 3138.03 | $9.24 \cdot 10^4$ | $2.87 \cdot 10^7$ | 105.79 |

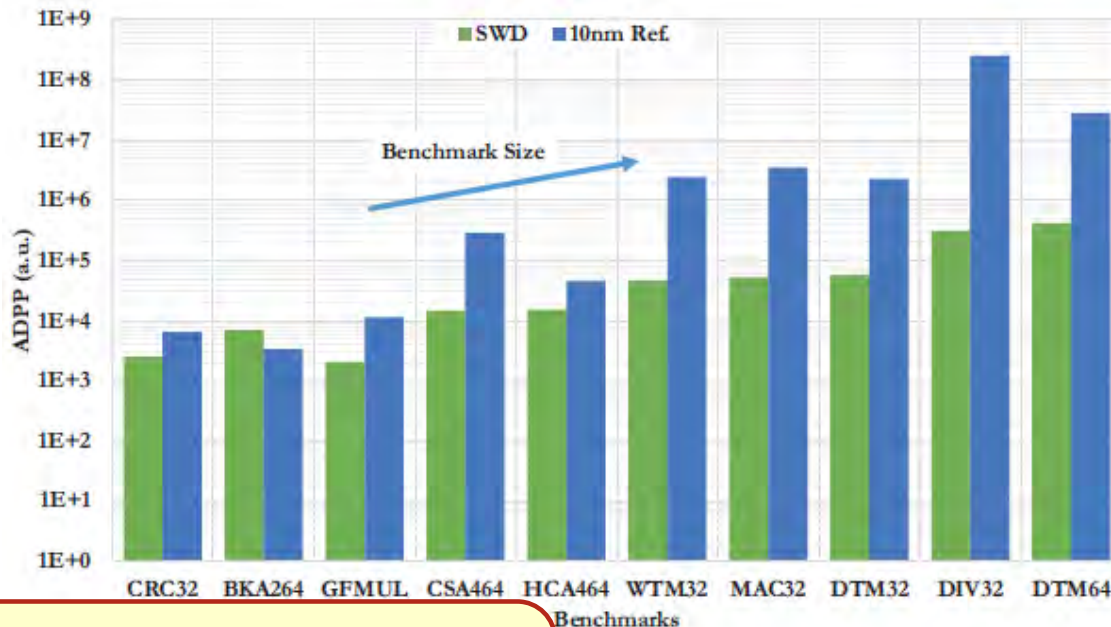
The list includes adders, multipliers,
a divider, and a cyclic redundancy check module

* Area-Delay-Power-Product (ADPP)

Zografos, et al., Proceedings of the 15th IEEE
International Conference on Nanotechnology
July 27-30, 2015, Rome, Italy

Benchmarking

Hybrid CMOS-Spin Wave Device Circuits Compared to 10nm CMOS



Area: 3.5x smaller
Delay: 10-20x slower
Power consumption: 100x lower
 ↓
ADPP: 50-100x better!

* Area-Delay-Power-Product (ADPP)

Zografos, et al., Proceedings of the 15th IEEE International Conference on Nanotechnology July 27-30, 2015, Rome, Italy

Computing principles

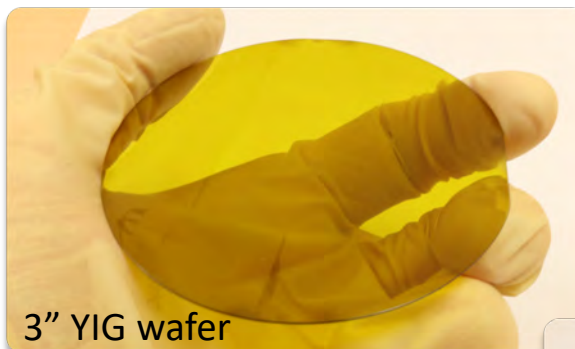


- Classical Computing
 - Scalar variable
 - Boolean logic
- Wave Packet Computing
 - Vector variable
 - Special task data processing
- Macroscopic Quantum State Computing
 - Vector state variable
- Quantum Computing
 - Vector state variable
 - Entanglement

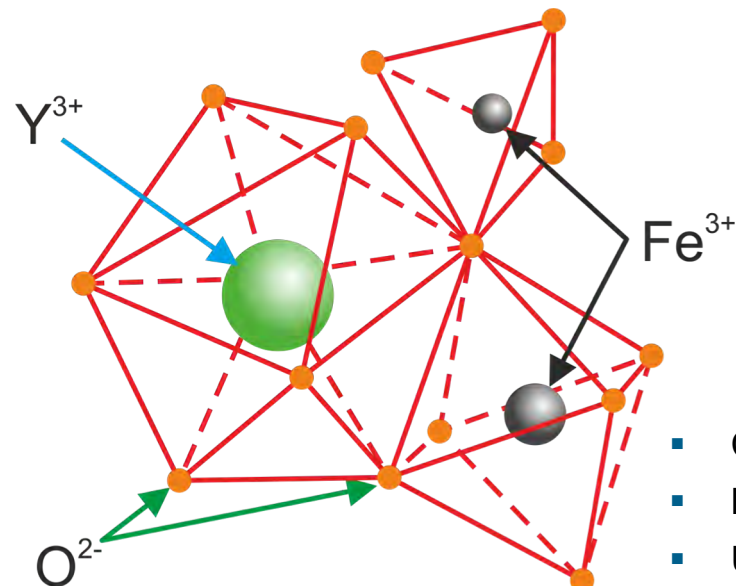
Quantum-Magnonic
Analogies

Yttrium Iron Garnet (YIG, $\text{Y}_3\text{Fe}_5\text{O}_{12}$)

- Room temperature ferrimagnet ($T_C = 560 \text{ K}$)
- Low phonon damping
- Magnon lifetime up to 700 ns !



Scientific Research Company
"Carat", Lviv, Ukraine



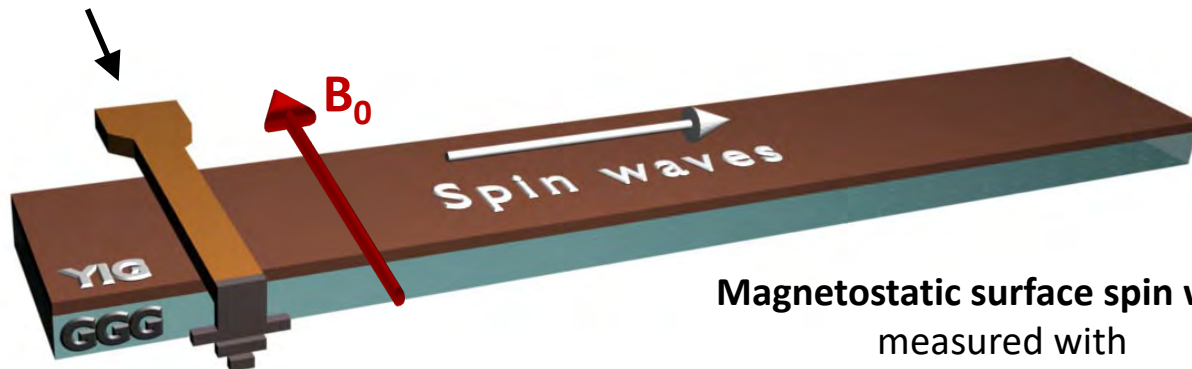
- Cubic crystal
- Lattice constant 12.376 Å
- Unit cell – 80 atoms

8 octahedral iron atoms (spin 5/2 up)
12 tetrahedral iron atoms (spin 5/2 down)

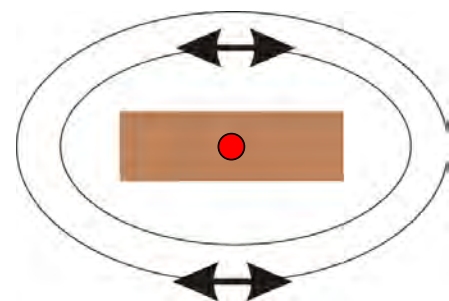
Magnetic moment of a unit cell is 20
Bohr magnetons μ_B at zero temperature

Excitation of dipolar spin waves

Input microwave signal

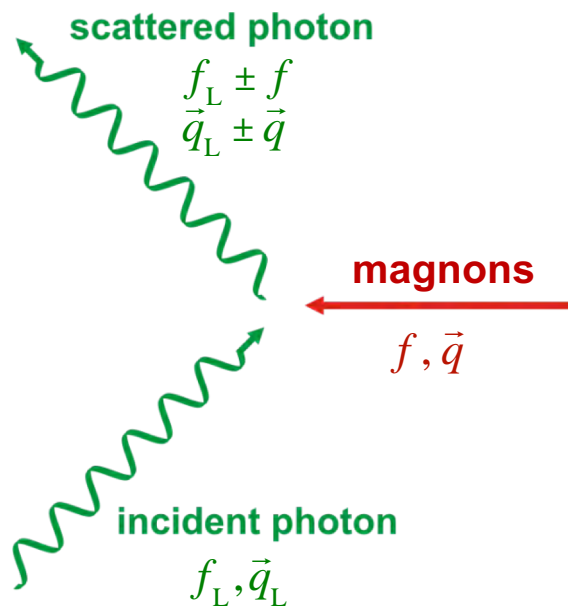


Magnetostatic surface spin waves
measured with
Brillouin light scattering spectroscopy



Alternating magnetic field

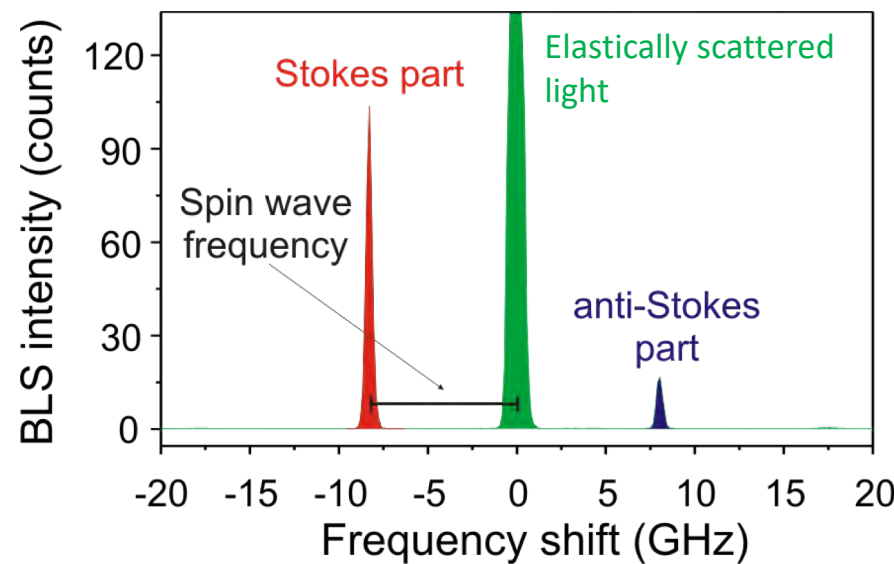
Brillouin light scattering spectroscopy



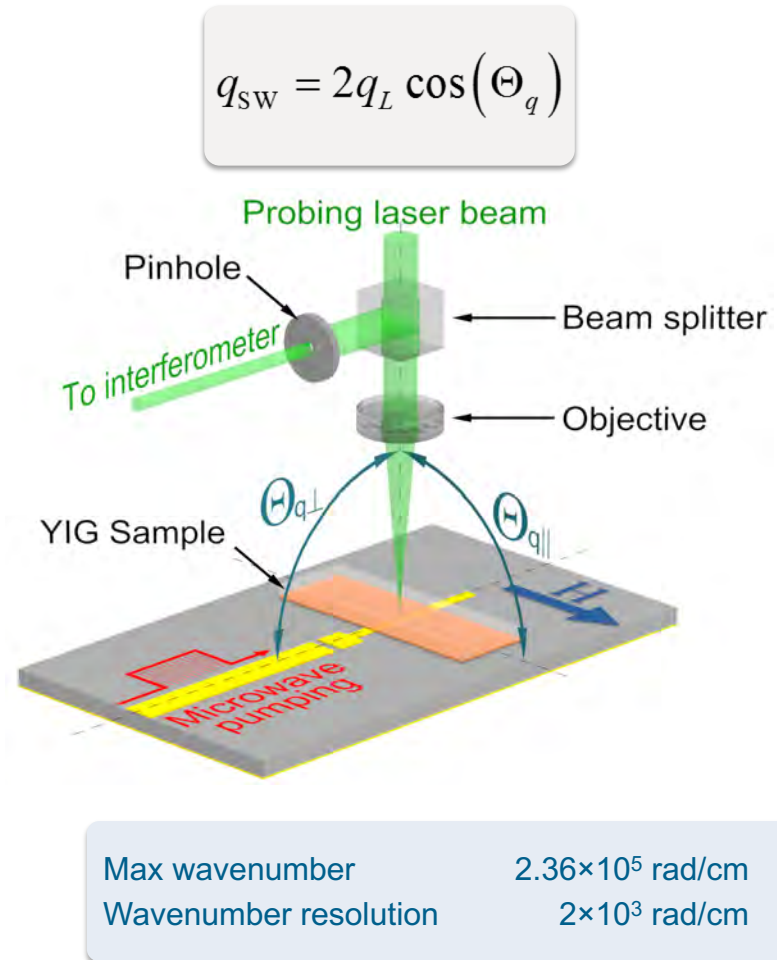
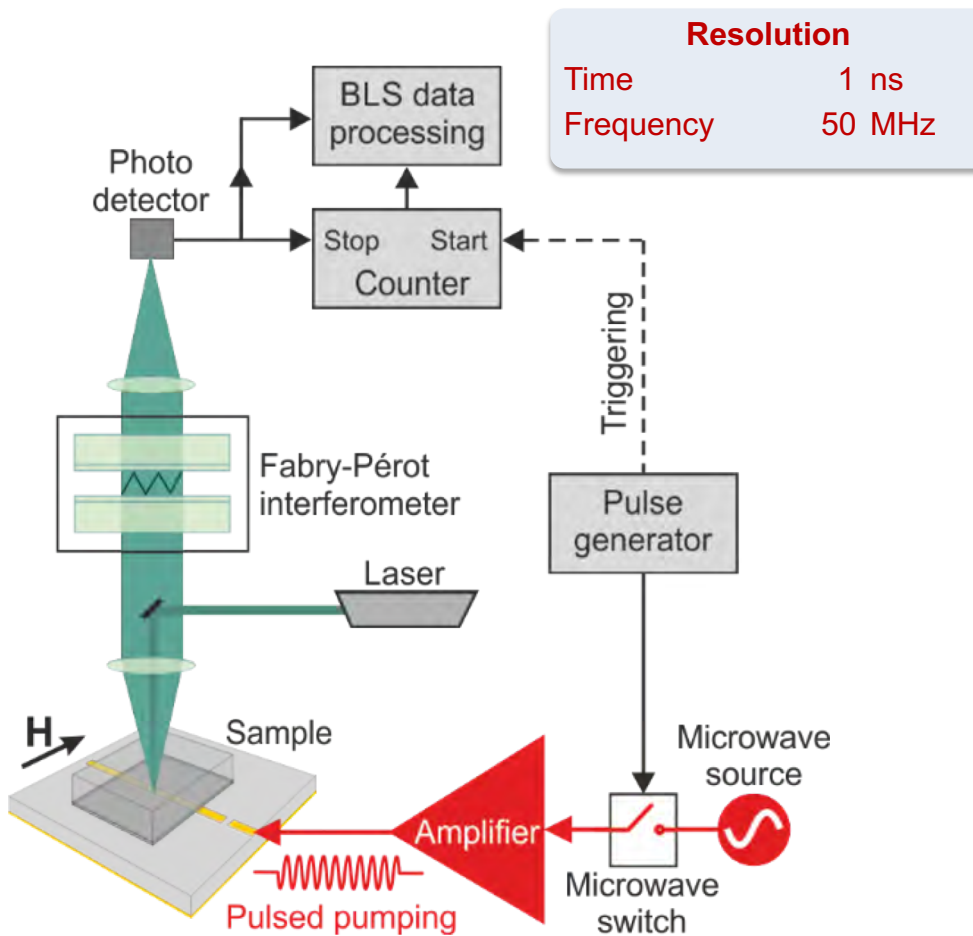
Brillouin light scattering process
= inelastic scattering of photons from spin waves

$$f_{\text{scattered L}} = f_L \pm f$$

$$\vec{q}_{\text{scattered L}} = \vec{q}_L \pm \vec{q}$$



Time-, space- and wavevector-resolved Brillouin light scattering spectroscopy



“Magnonics” team

Kaiserslautern PI Team



A. Chumak



P. Pirro



T. Brächer



V. Vasyuchka



A. Serga

Main External Collaborators

V.S. L'vov (Weizmann Institute of Science, Rehovot, Israel)

G.A. Melkov (National Taras Shevchenko University of Kyiv, Ukraine)

E. Saitoh (Tohoku University, Sendai, Japan)

A.N. Slavin (Oakland University, Rochester, USA)

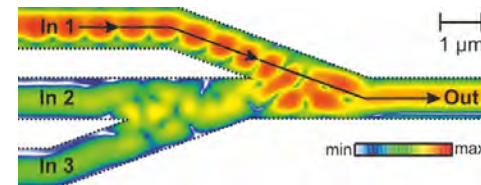
AG Magnetismus



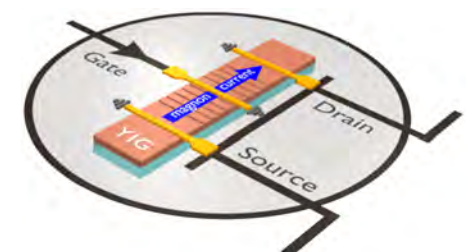
Prof. B. Hillebrands, Jun. Prof. A. V. Chumak, V. Lauer, Q. Wang, P. Frey, B. Heinz, L. Mihalceanu, M. Kewenig,
Dr. D. A. Bozhko, M. Schneider, Dr. P. Pirro, M. Schweizer, Dr. habil. A. A. Serga, Dr. T. Langner, E. Wiedemann,
A. Kreil, Dr. A. Conca Parra, S. Steinert, M. Geilen, S. Keller, H. Schäfer, T. Noack, T. Fischer, Dr. T. Meyer,
Jun. Prof. E. Th. Papaioannou, F. Heussner, J. Greser, K. Fukuda (guest), Dr. V. I. Vasyuchka

Advanced magnonics

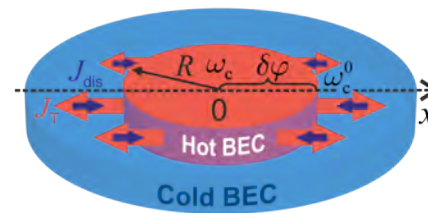
I. Magnon interference logic



II. Non-linear magnonics: Magnon transistor

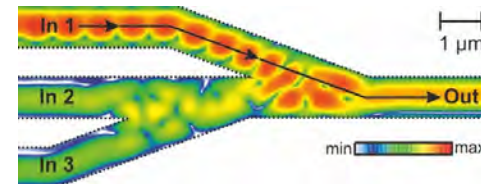


III. Magnonic macroscopic quantum state

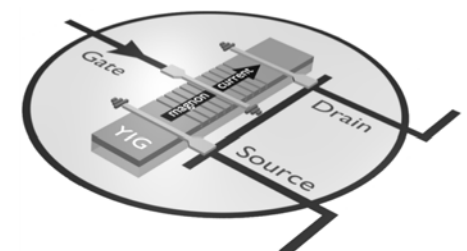


Advanced magnonics

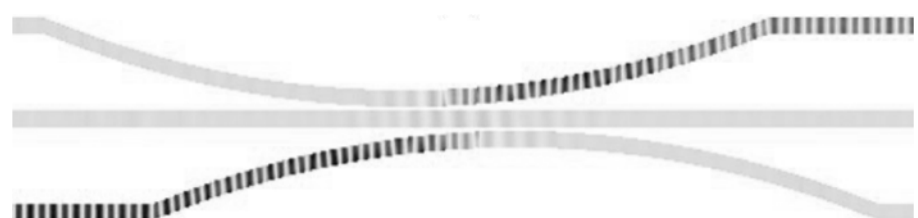
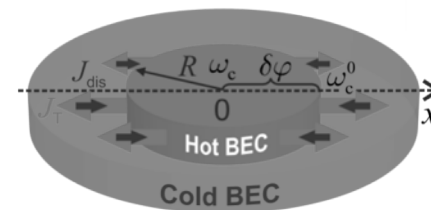
I. Magnon interference logic



II. Non-linear magnonics: Magnon transistor

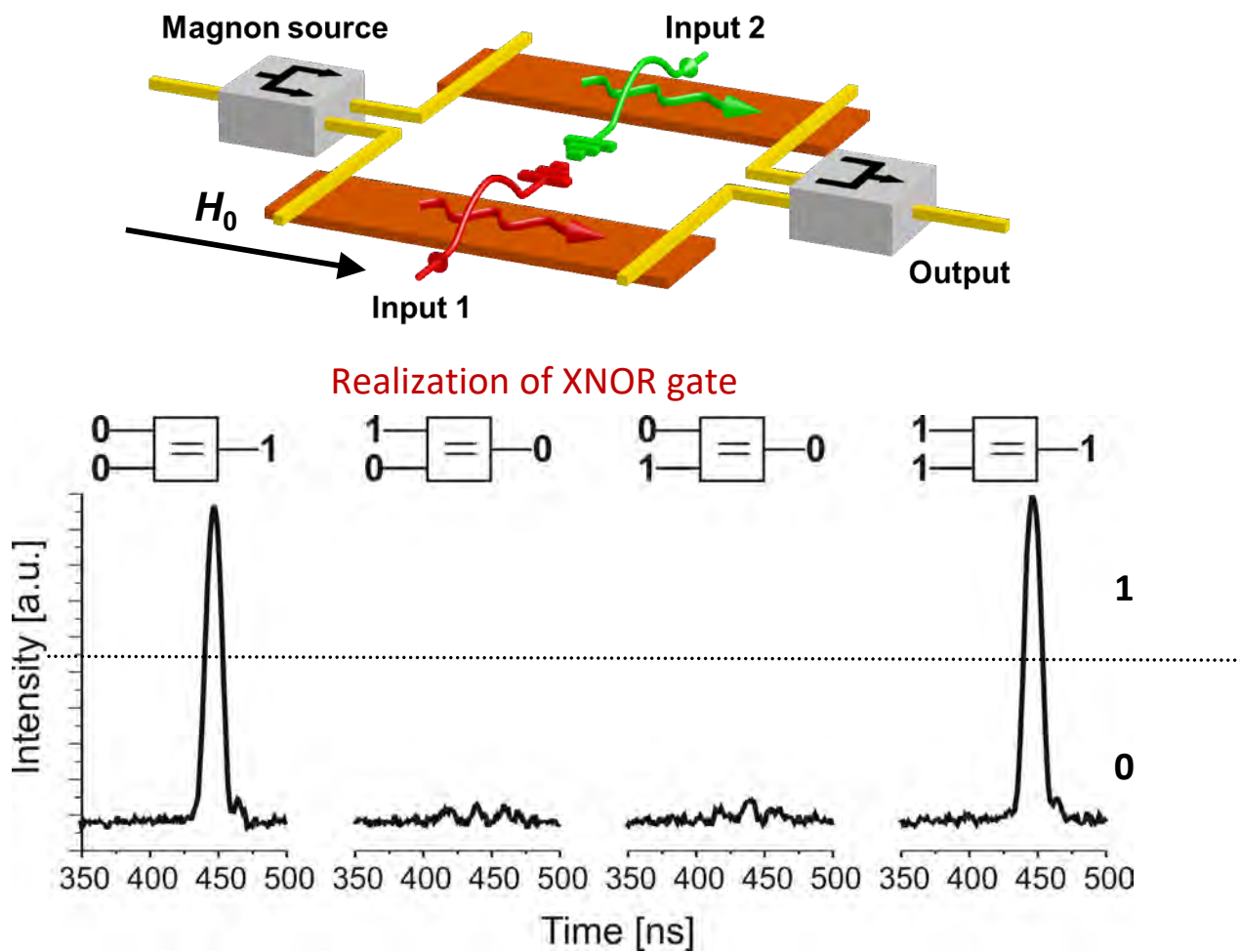


III. Magnonic macroscopic quantum state



IV. Quantum-classical analogies in magnonics

First prototype Mach-Zehnder interferometer based spin-wave logic gate



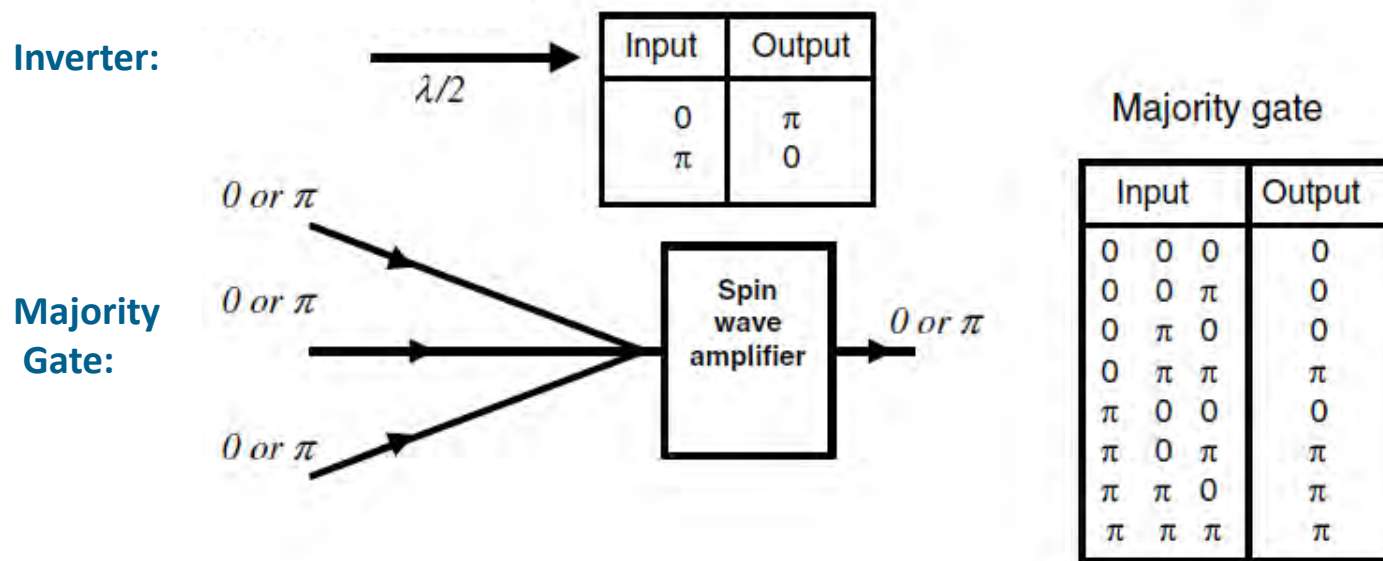
| Inputs | | Output |
|---------------|---------------|--------|
| A (I_1) | B (I_2) | |
| 0 (0) | 0 (0) | 1 |
| 0 (0) | 1 (I_π) | 0 |
| 1 (I_π) | 0 (0) | 0 |
| 1 (I_π) | 1 (I_π) | 1 |

Kostylev et al., APL **87**, 153501 (2005)

Schneider et al., APL **92**, 022505 (2008)

Magnon majority gates: General idea

Data is coded into spin-wave phase

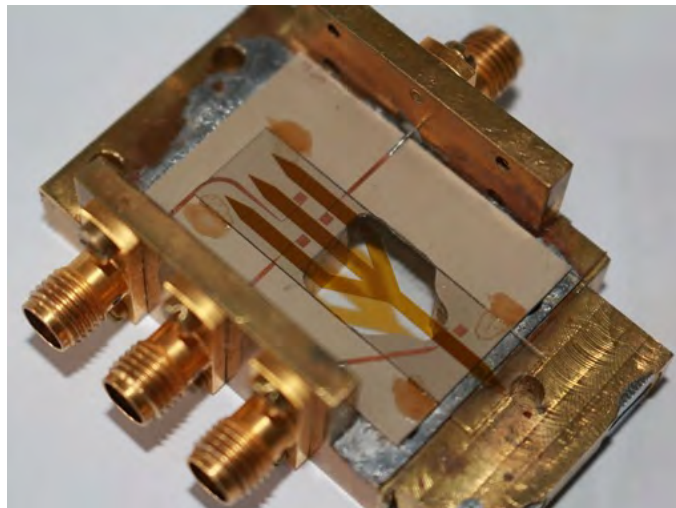


A. Khitun, et al., J. Phys. D. **43**, 264005 (2010)

- simple realization of majority gate (spin-wave combiner)
- trivial realization of NOT operation (= phase shift during $\Delta x = \lambda/2$ propagation)
- is all-magnonic
- majority gate + inverter are building blocks for full logic functionality

Experimental realization

Macroscopic majority gate



YIG sample:

- thickness 5.4 μm
- waveguide width 1.5 mm

Geometry

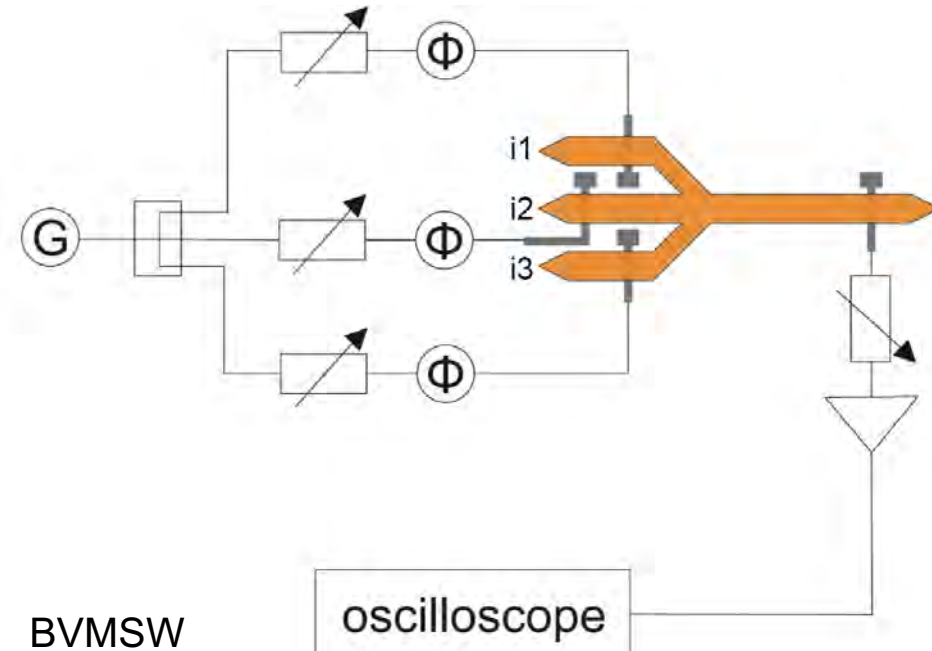
- Frequency
- Magnetic field

BVMSW

- 6.035 GHz
- 1429 Oe

Produced by Scientific Research
Company Carat, Lviv, Ukraine

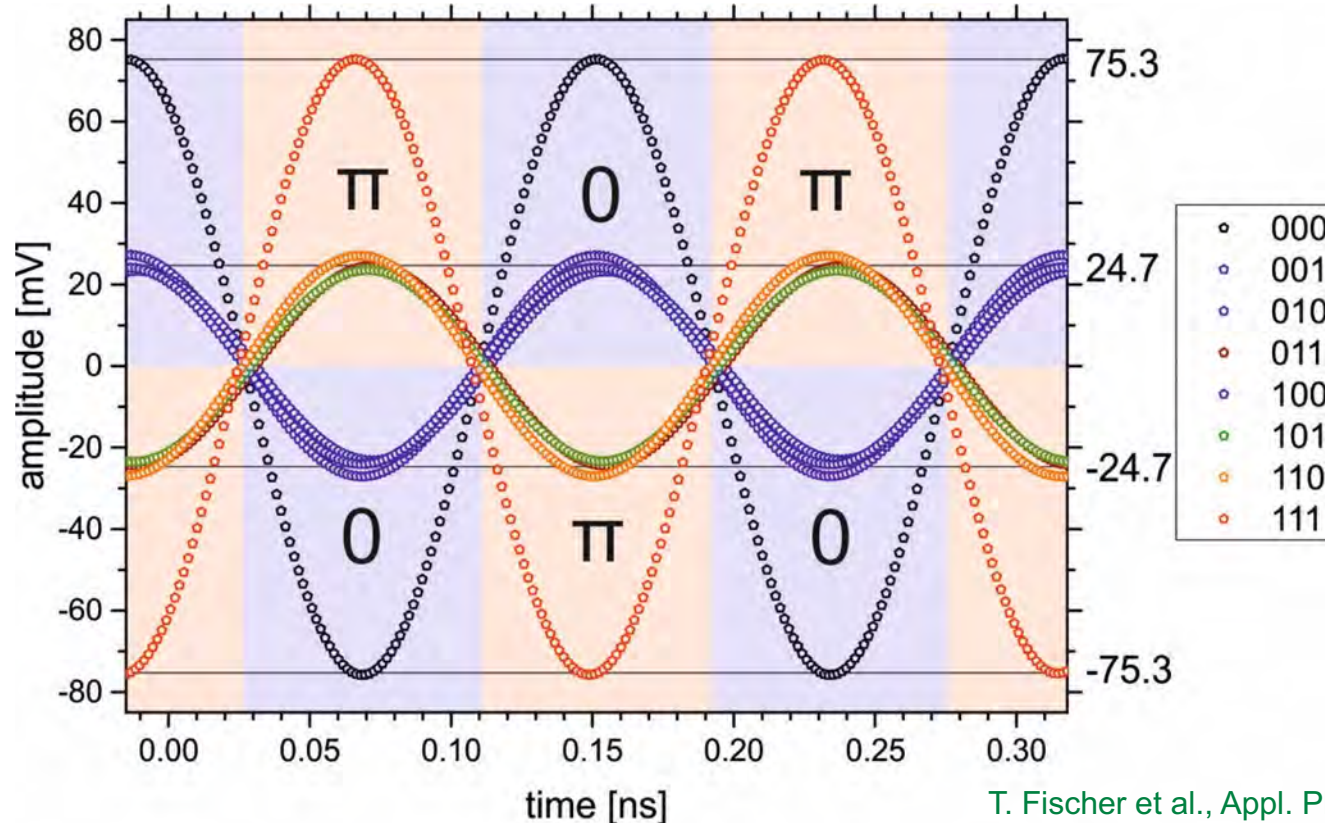
Experimental setup



oscilloscope

T. Fischer et al., Appl. Phys. Lett. **110**, 152401 (2017)

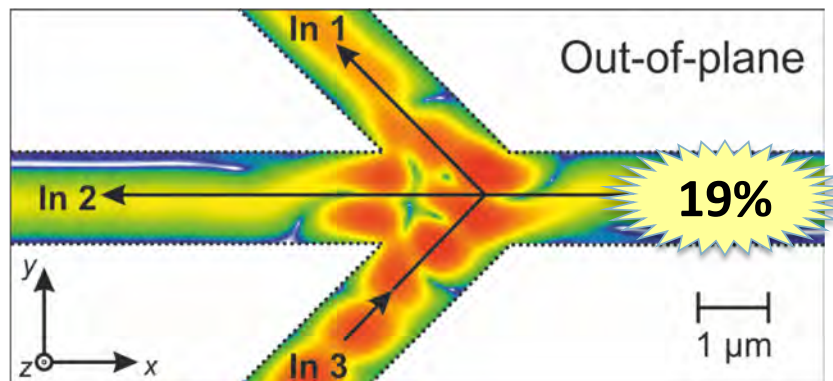
Superposition of all spin-wave channels



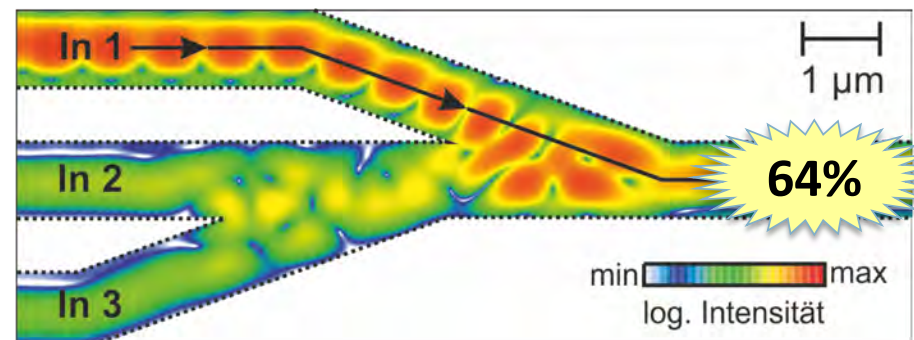
T. Fischer et al., Appl. Phys. Lett. **110**, 152401 (2017)

The output phase of the signal is defined by the majority of the input phases

Majority gates: Out-of-plane magnetization



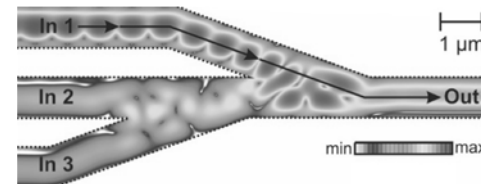
How to increase
this value?



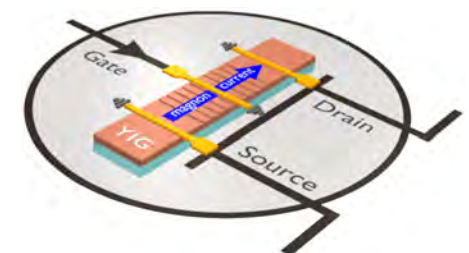
S. Klingler et al., Appl. Phys. Lett. **106**, 212406 (2015)

Advanced magnonics

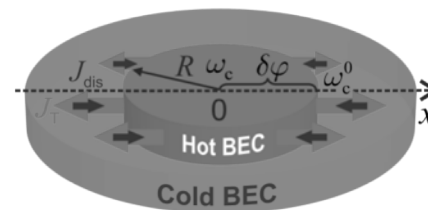
I. Magnon interference logic



II. Non-linear magnonics: Magnon transistor



III. Magnonic macroscopic quantum state



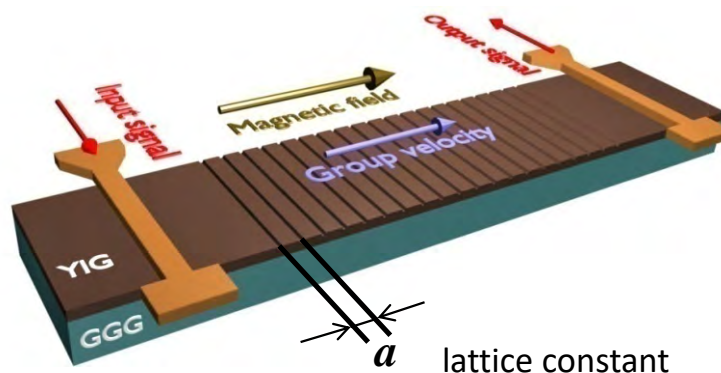
IV. Quantum-classical analogies in magnonics

Magnonic crystal

Magnonic crystal – magnetic meta-material:

- artificial medium with periodic lateral variation in magnetic properties
- Acts like magnonic Fabry-Pérot cavity characterized by quality factor

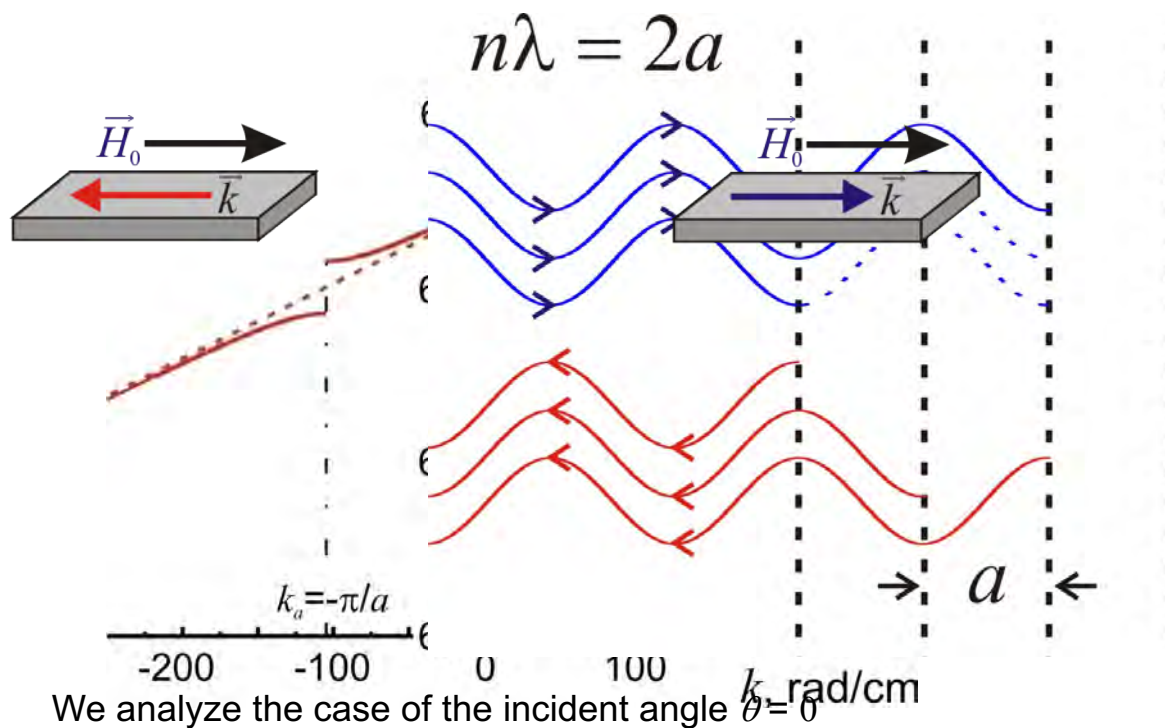
One-dimensional magnonic crystal:



- analogous to **photonic and sonic** crystals but operates with spin waves in the GHz frequency range

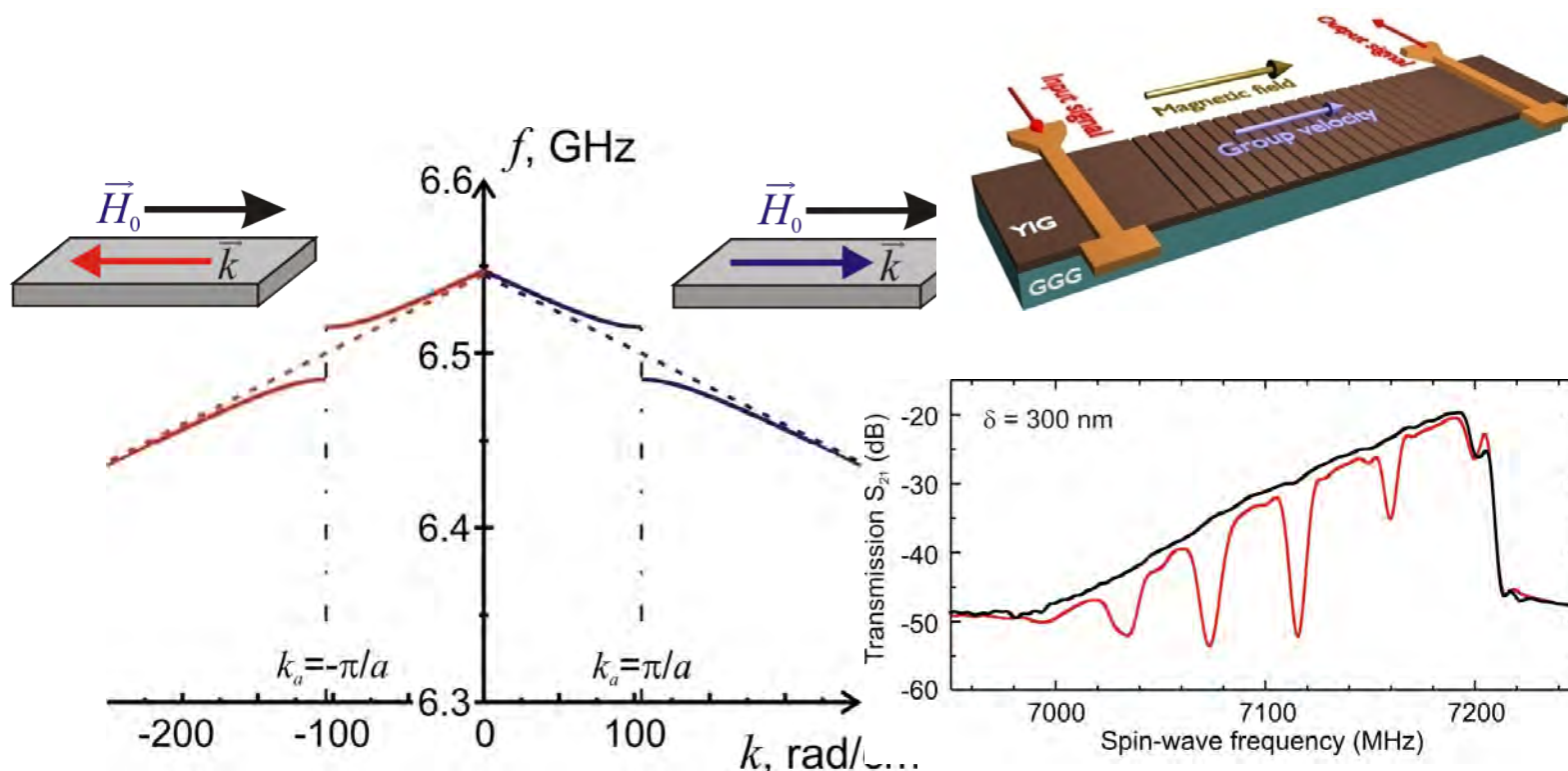
Band gap

Band gaps – regions of the spectrum over which waves are **not allowed** to propagate



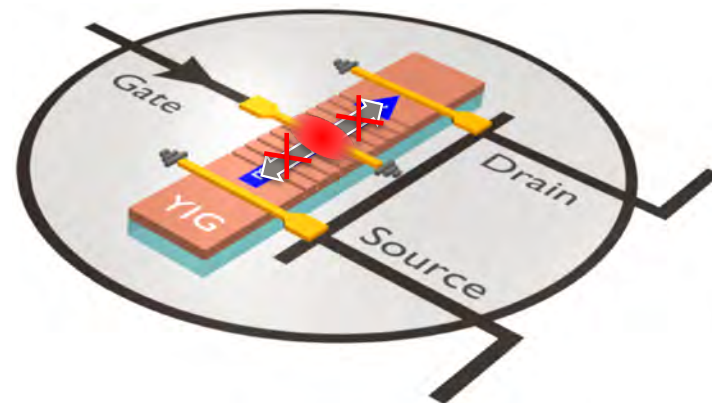
Band gap

Band gaps – regions of the spectrum over which waves are **not allowed** to propagate

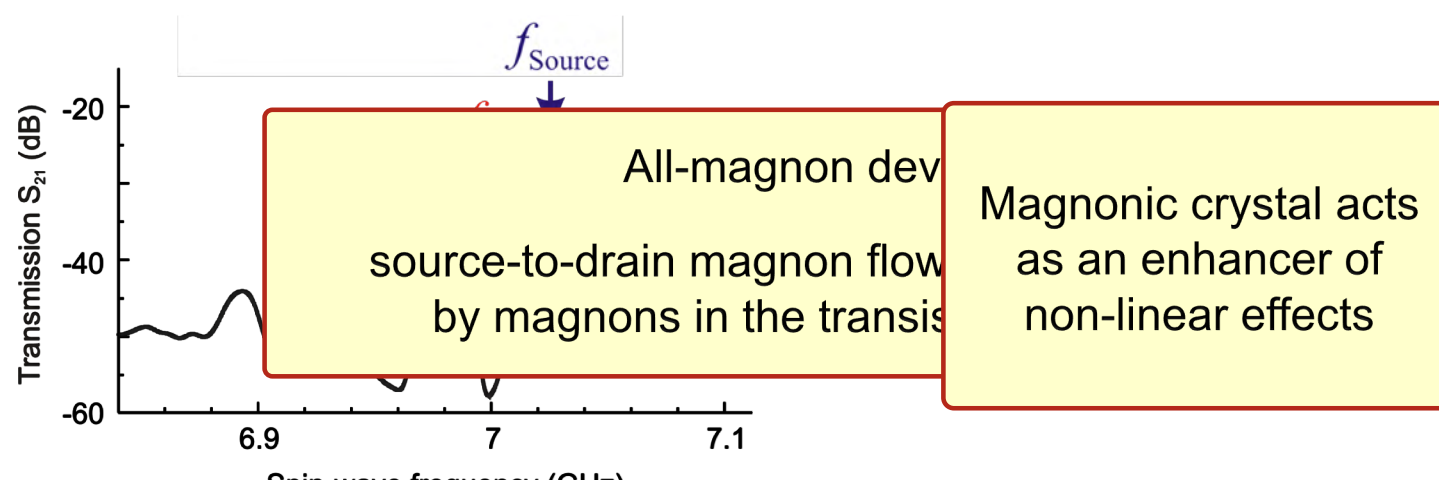
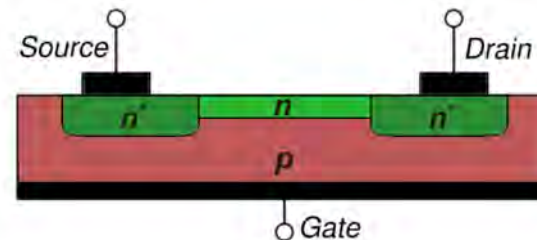


A.V. Chumak et al., Appl. Phys. Lett. **93**, 022508 (2008)

Magnon transistor



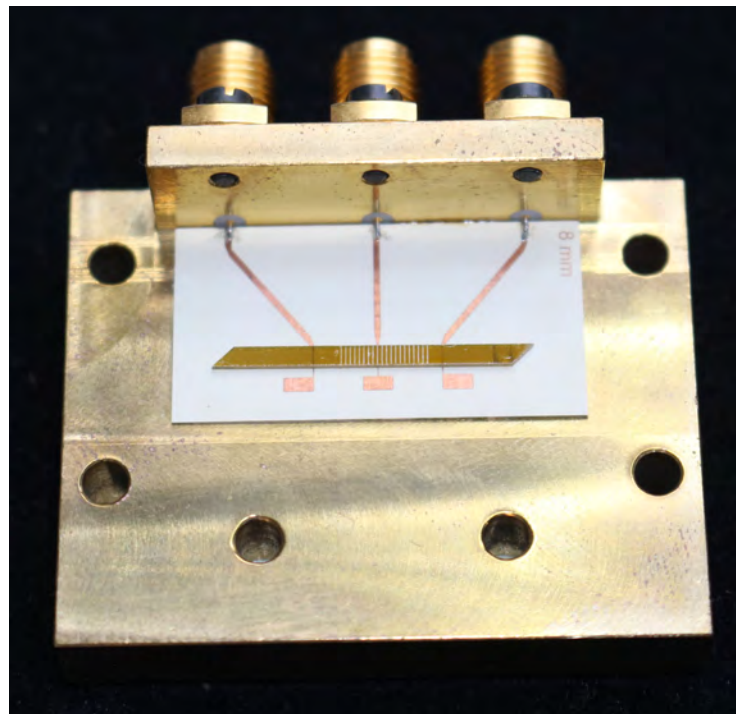
Semiconductor field-effect transistor:



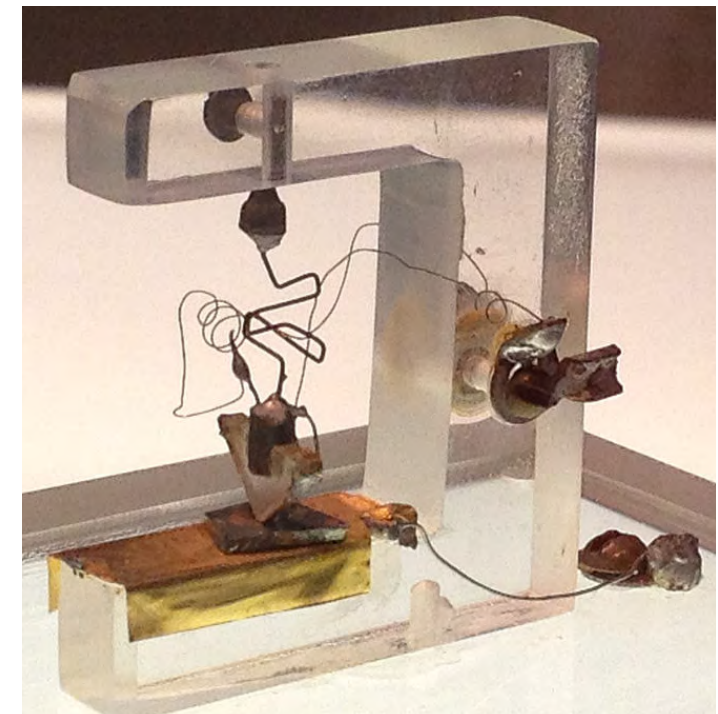
A.V. Chumak et al., Nat. Commun. 5:4700 (2014)

First transistors

Magnon transistor prototype, 2014



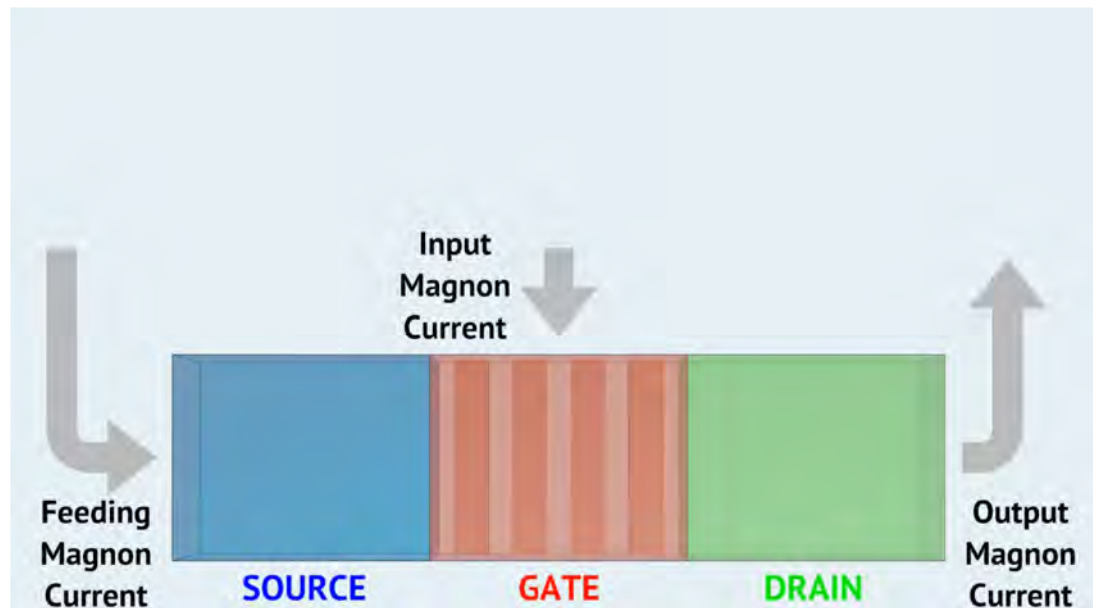
First transistor, 1947



<https://de.wikipedia.org>

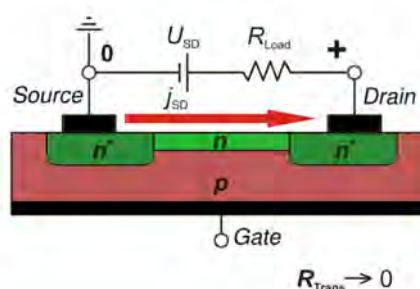
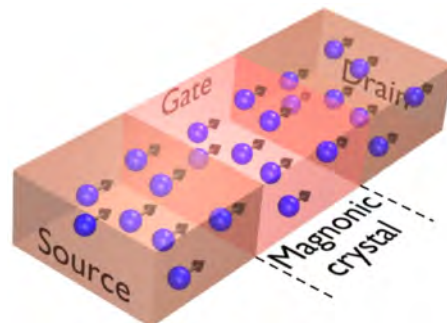
Magnon transistor

Magnon transistor allows for the control of one magnon current by another

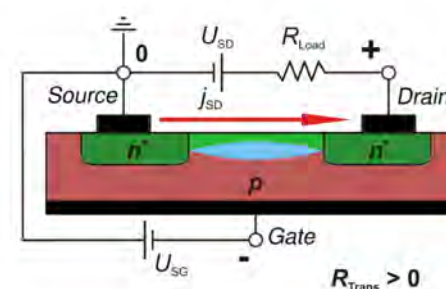
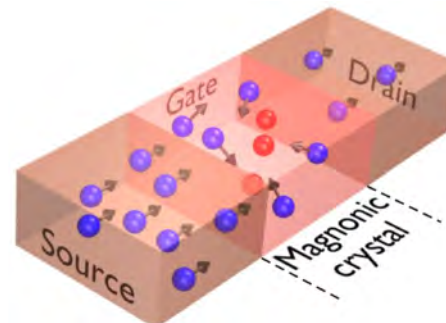


Magnon transistor

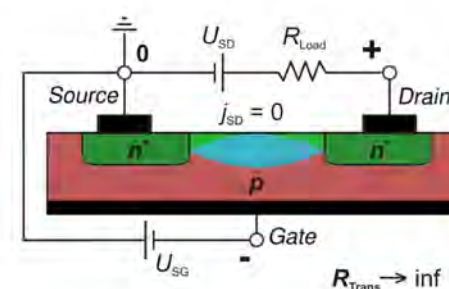
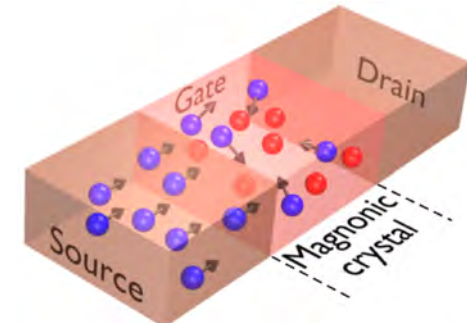
Opened: $R \rightarrow 0$
Gate magnon density
 $n_G = 0$



Semi-closed: $R > 0$
Gate magnon density
 $n_G > 0$



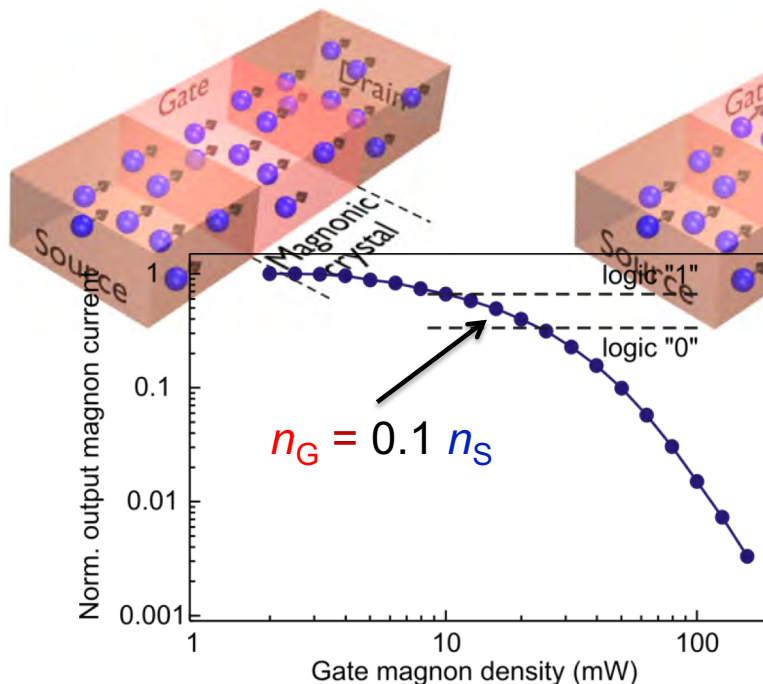
Closed: $R \rightarrow \infty$
Gate magnon density
 $n_G \gg 0$



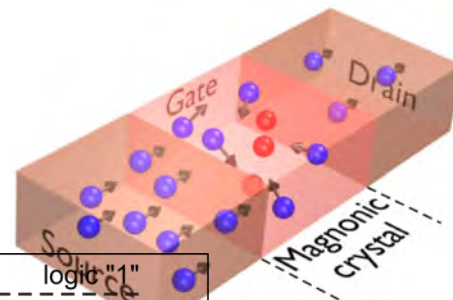
A.V. Chumak et al., Nat. Commun. 5:4700 (2014)

Magnon transistor

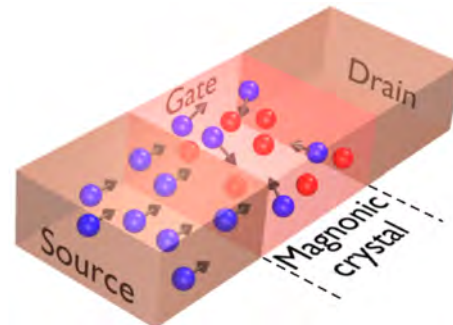
Opened: $R \rightarrow 0$
Gate magnon density
 $n_G = 0$



Semi-closed: $R > 0$
Gate magnon density
 $n_G > 0$



Closed: $R \rightarrow \infty$
Gate magnon density
 $n_G \gg 0$

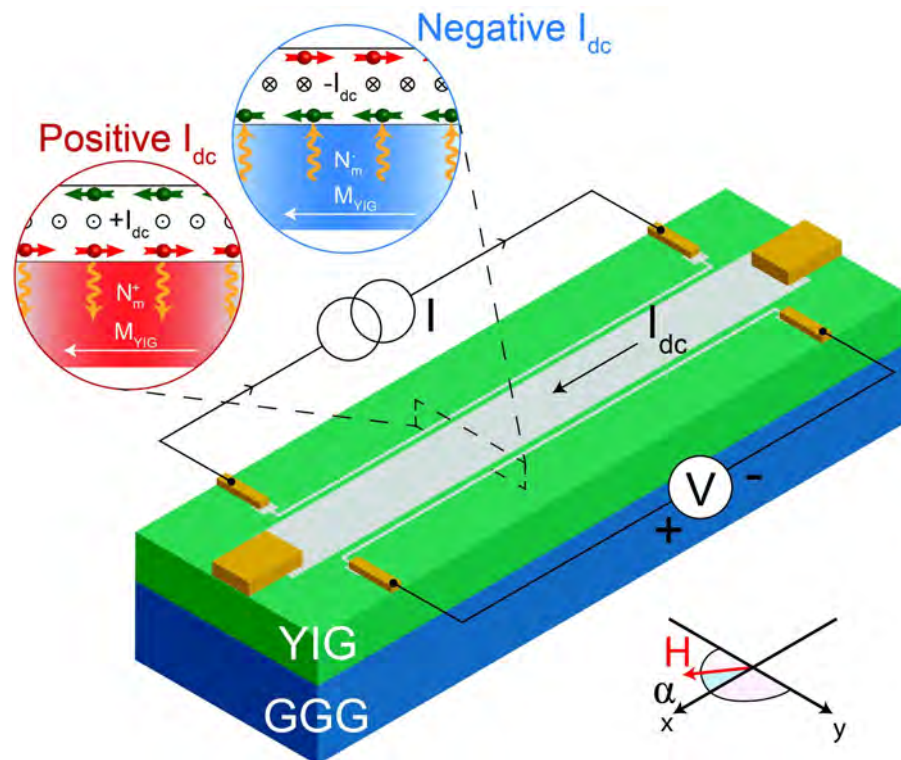


“magnon control by magnon” principle was realized:
data can be processed on the same magnetic chip

A.V. Chumak et al., Nat. Commun. 5:4700 (2014)

Magnon transistor based on the diffusive transport of thermal magnons

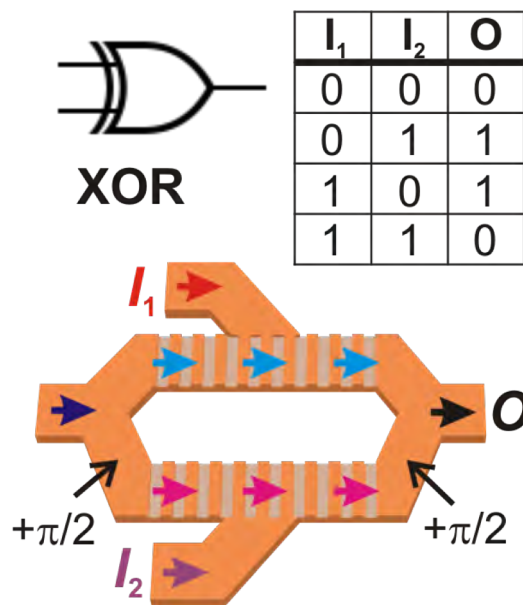
Proof of principle of a method for modulating the diffusive transport of thermal magnons



L. J. Cornelissen et al., Phys. Rev. Lett. **120**, 097702 (2018)

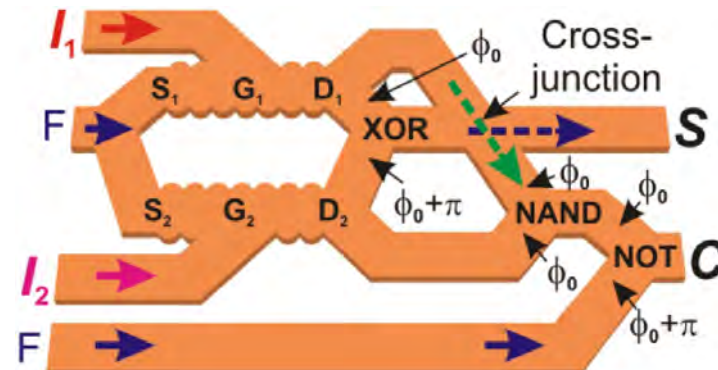
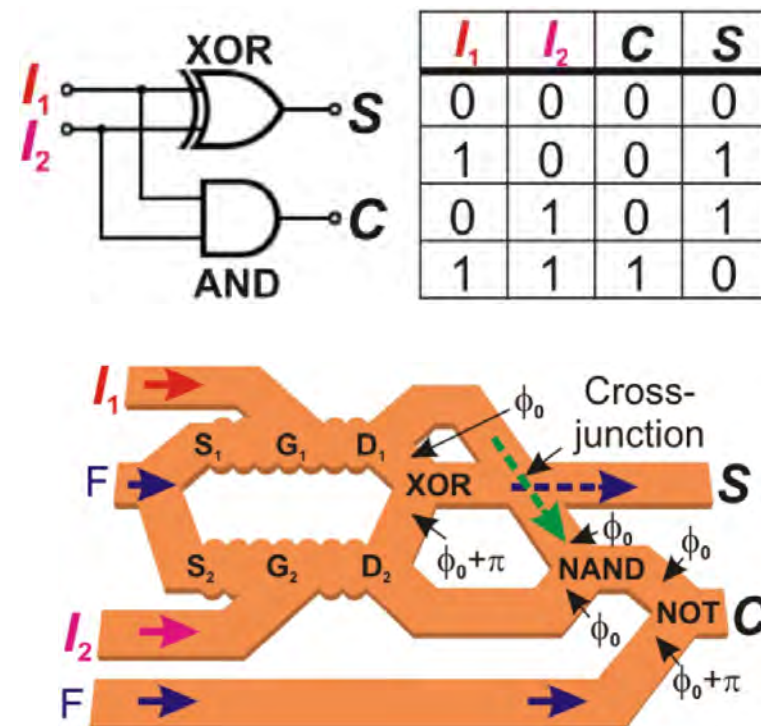
Logic operations

XOR logic gate



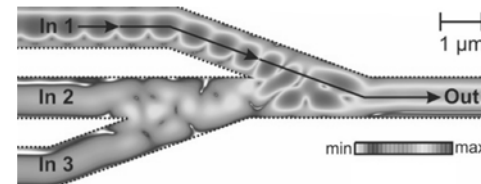
XOR gate requires 2 magnon transistors instead of 8 FET in CMOS

Half adder

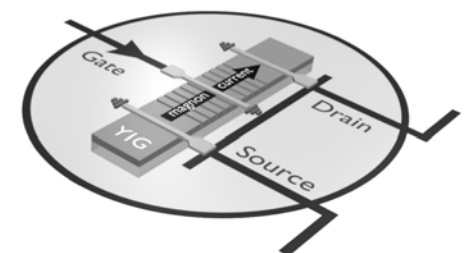


Advanced magnonics

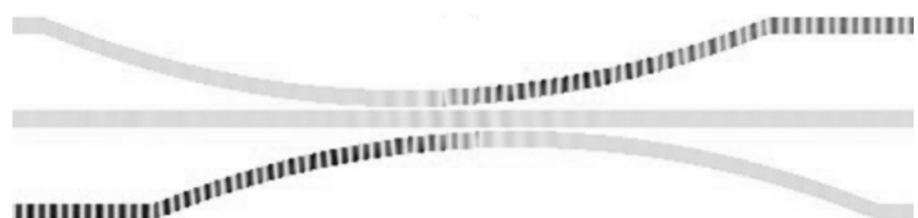
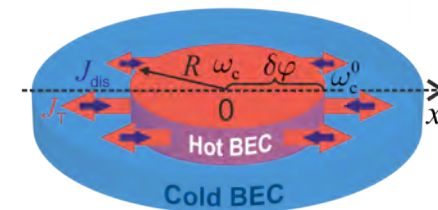
I. Magnon interference logic



II. Non-linear magnonics: Magnon transistor



III. Magnonic macroscopic quantum state



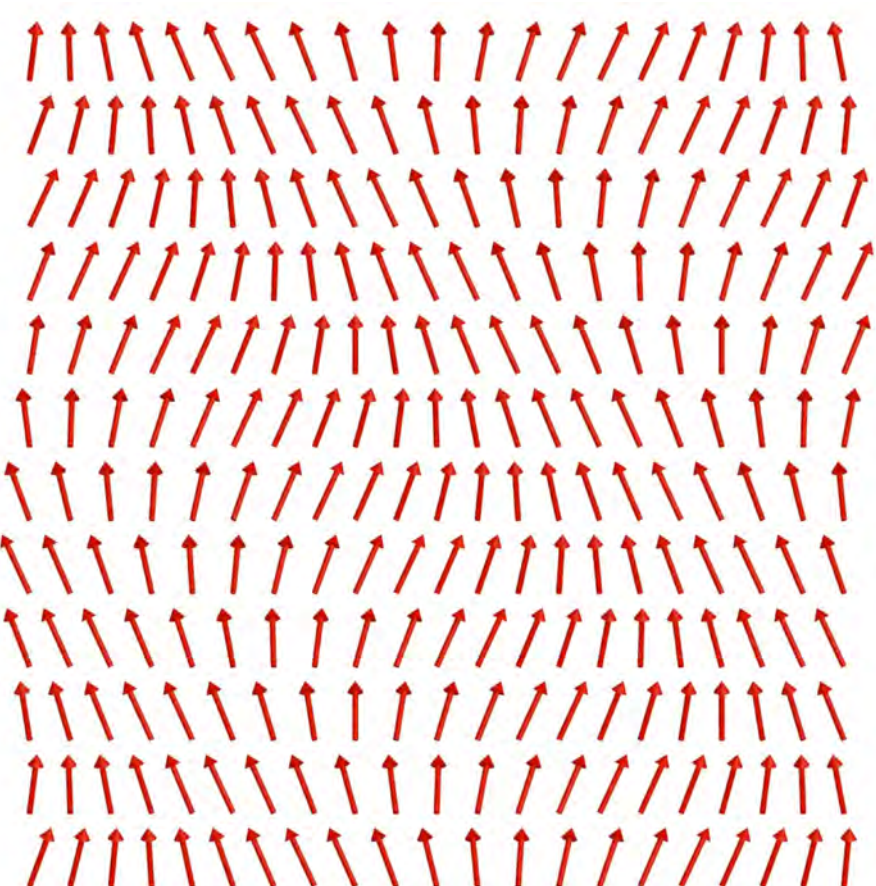
IV. Quantum-classical analogies in magnonics

Magnon as a quanta of spin-wave

- Energy $\varepsilon = \hbar \omega = \frac{\eta}{\hbar} p^2$
- Momentum $\vec{p} = \hbar \vec{q}$
- Mass $m = \hbar / (2\eta)$
- Spin $s = 1$
- Four- and three-magnon scattering



Magnon gas



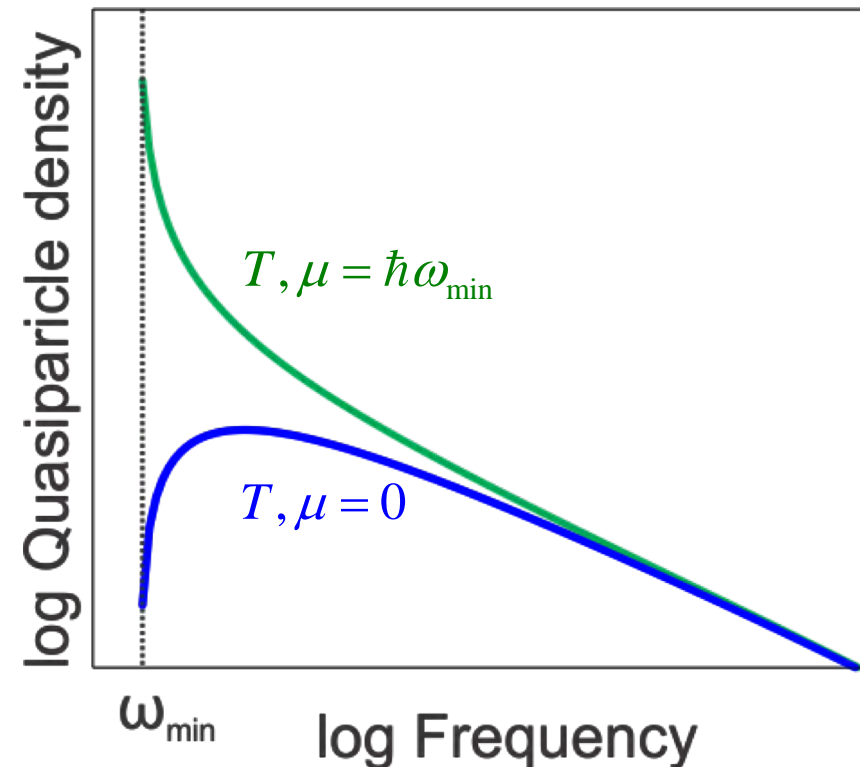
Magnon distribution

Bose-Einstein distribution

$$\rho(\omega) = \frac{D(\omega)}{\exp\left(\frac{\hbar\omega - \mu}{k_B T}\right) - 1}$$

μ : chemical potential

Magnons are **bosons** ($s=1$) and similar to other quasi-particles are described **in thermal equilibrium** by Bose-Einstein distribution with **zero chemical potential**



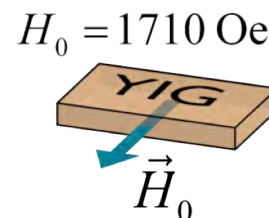
Magnon spectrum of in-plane magnetized YIG film

$$\frac{\partial \vec{M}}{\partial t} = -|\gamma| \vec{M} \times \vec{H}_{\text{eff}}$$

Landau-Lifshitz equation

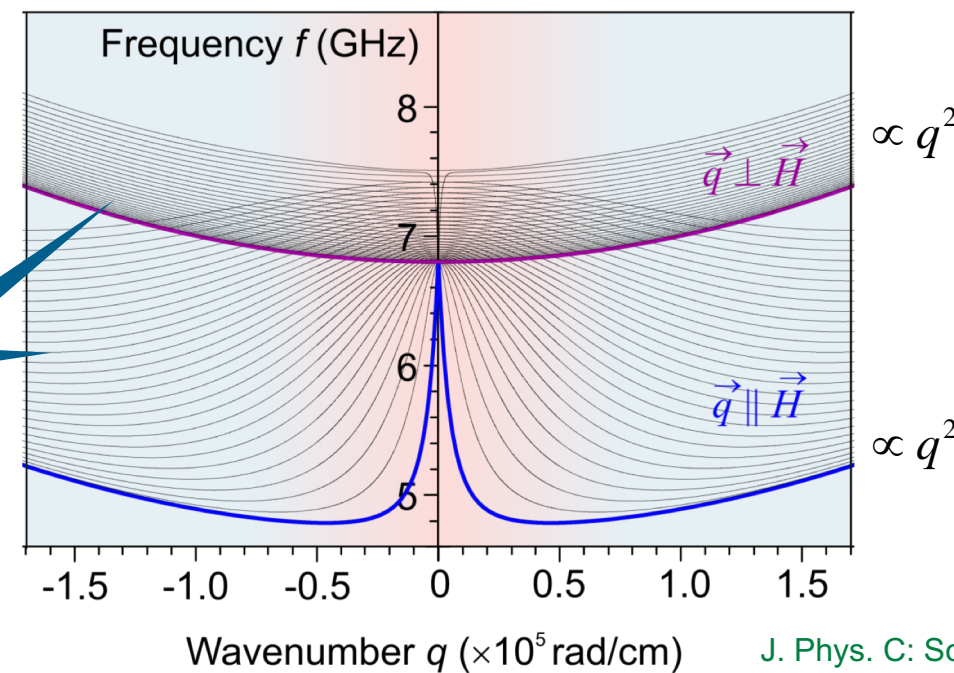
$$\vec{H}_{\text{eff}}(\vec{r}) = \vec{H}_0 + \int_V \tilde{G}(\vec{r}, \vec{r}') \cdot \vec{M}(\vec{r}') d\vec{r}'^3 + \frac{\eta}{\gamma M_S} \nabla^2 \vec{M} + \dots$$

dipolar interaction exchange interaction



Thickness modes having a non-uniform harmonic distribution of dynamic magnetization along the film thickness

6 μm thick YIG film

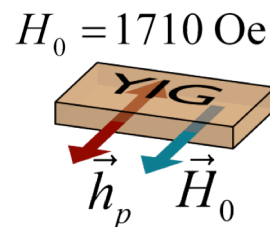


Calculations based on:
Kalinikos and Slavin,
J. Phys. C: Solid State Phys **19**, 7013 (1986)

Control of magnon gas density by parametric pumping

Energy and momentum conservation laws for parametric pumping

$$\begin{cases} \vec{q}_{\text{sw}} + \vec{q}'_{\text{sw}} = \vec{q}_p \approx 0 \\ f_{\text{sw}} + f'_{\text{sw}} = f_p \end{cases}$$

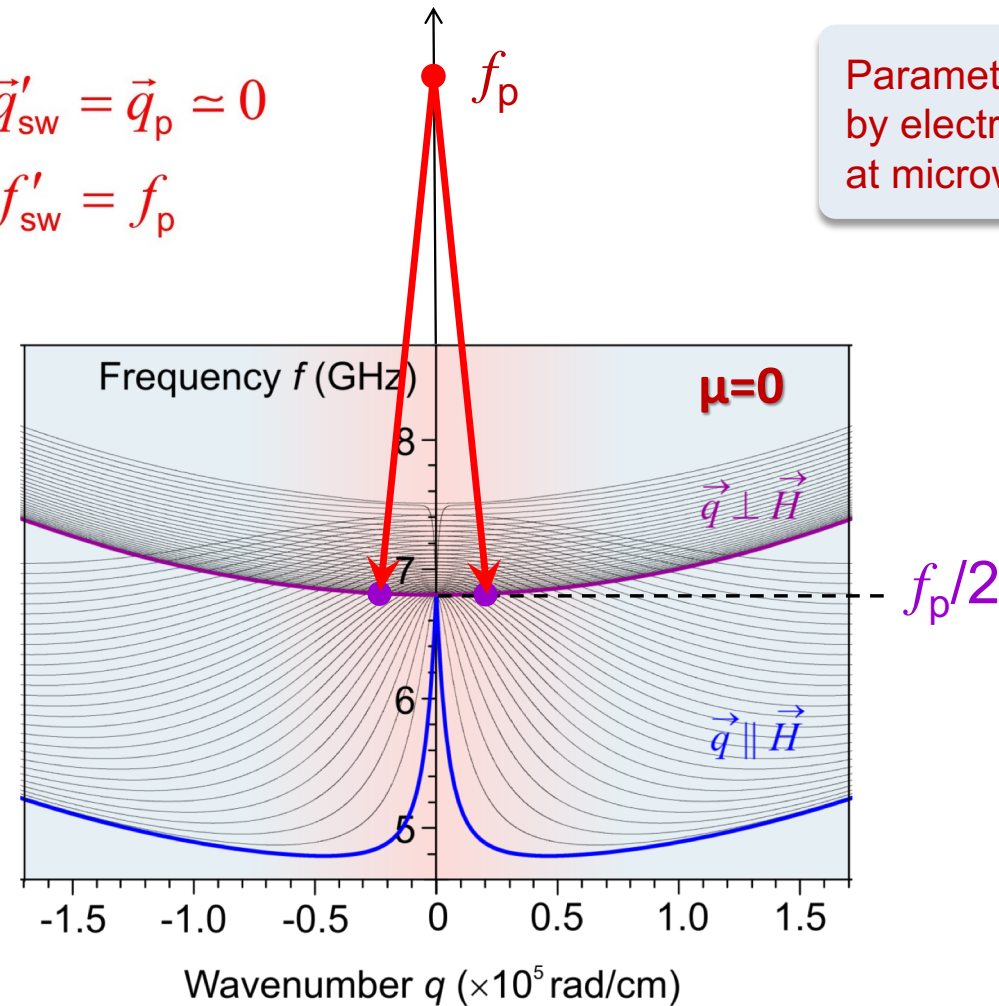


Bose-Einstein distribution

$$\rho(f) = \frac{D(f)}{\exp\left(\frac{hf - \mu}{k_B T}\right) - 1}$$

μ : chemical potential

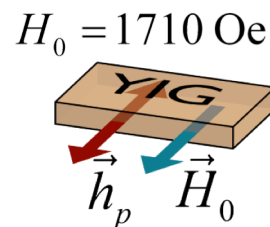
Parametric pumping by electromagnetic wave at microwave frequency



Control of magnon gas density by parametric pumping

Energy and momentum conservation laws for parametric pumping

$$\begin{cases} \vec{q}_{\text{sw}} + \vec{q}'_{\text{sw}} = \vec{q}_p \approx 0 \\ f_{\text{sw}} + f'_{\text{sw}} = f_p \end{cases}$$

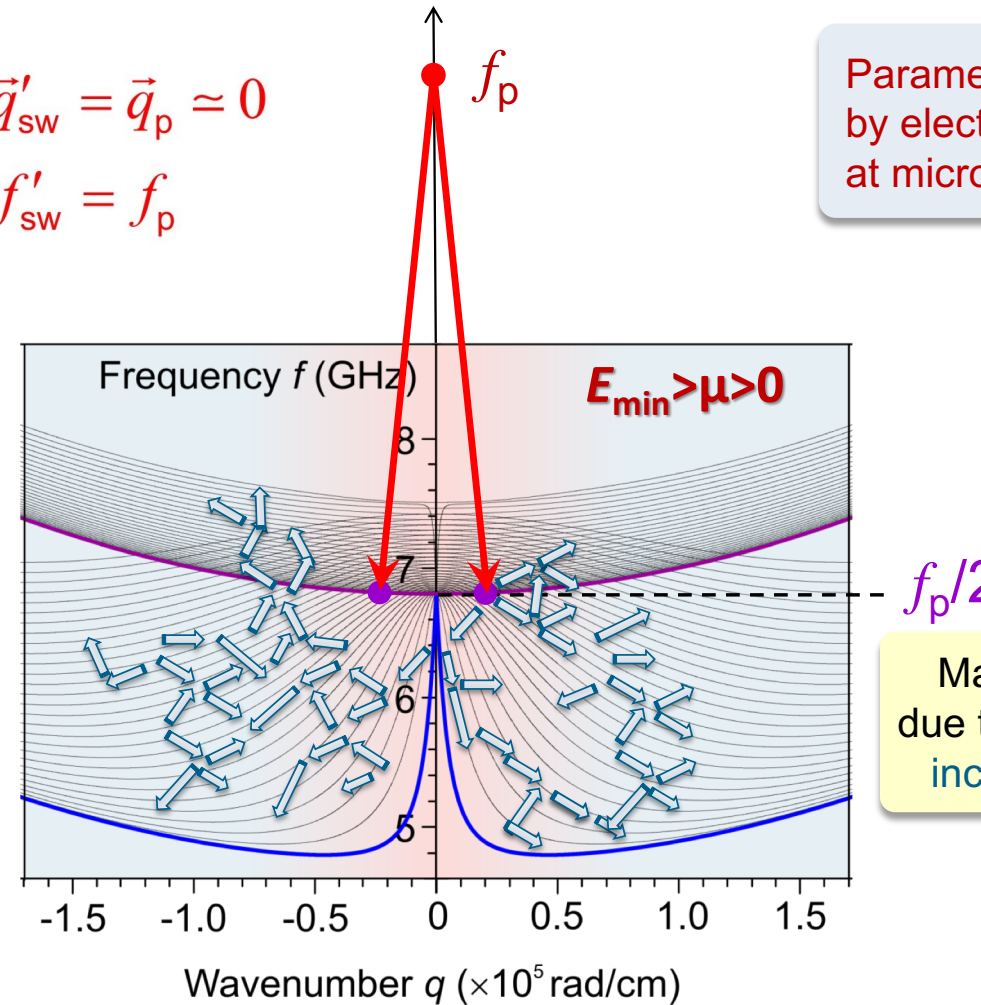


Bose-Einstein distribution

$$\rho(f) = \frac{D(f)}{\exp\left(\frac{hf - \mu}{k_B T}\right) - 1}$$

μ : chemical potential

Parametric pumping by electromagnetic wave at microwave frequency



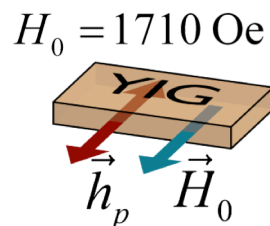
$f_p/2$

Magnon thermalization due to 4-particle scattering:
incoherent magnon gas

Bose-Einstein condensation of magnons

Energy and momentum conservation laws for parametric pumping

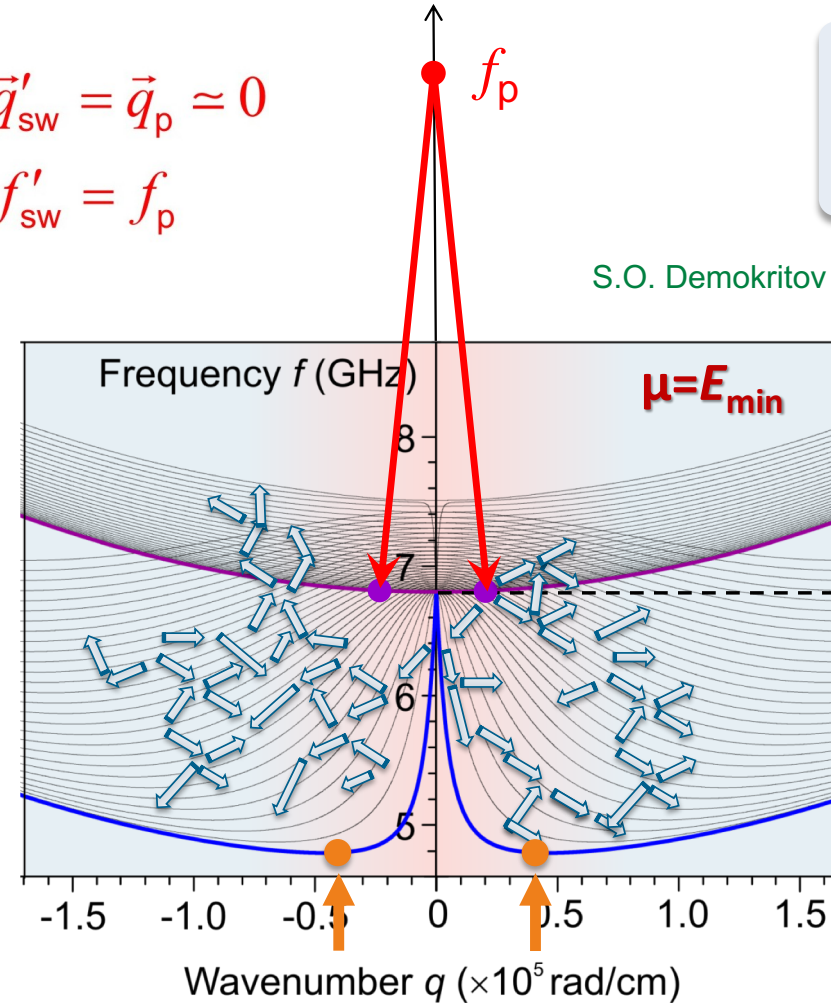
$$\begin{cases} \vec{q}_{\text{sw}} + \vec{q}'_{\text{sw}} = \vec{q}_p \approx 0 \\ f_{\text{sw}} + f'_{\text{sw}} = f_p \end{cases}$$



Bose-Einstein distribution

$$\rho(f) = \frac{D(f)}{\exp\left(\frac{hf - \mu}{k_B T}\right) - 1}$$

μ : chemical potential



Parametric pumping by electromagnetic wave at microwave frequency

S.O. Demokritov *et al.*, Nature 443, 430 (2006)

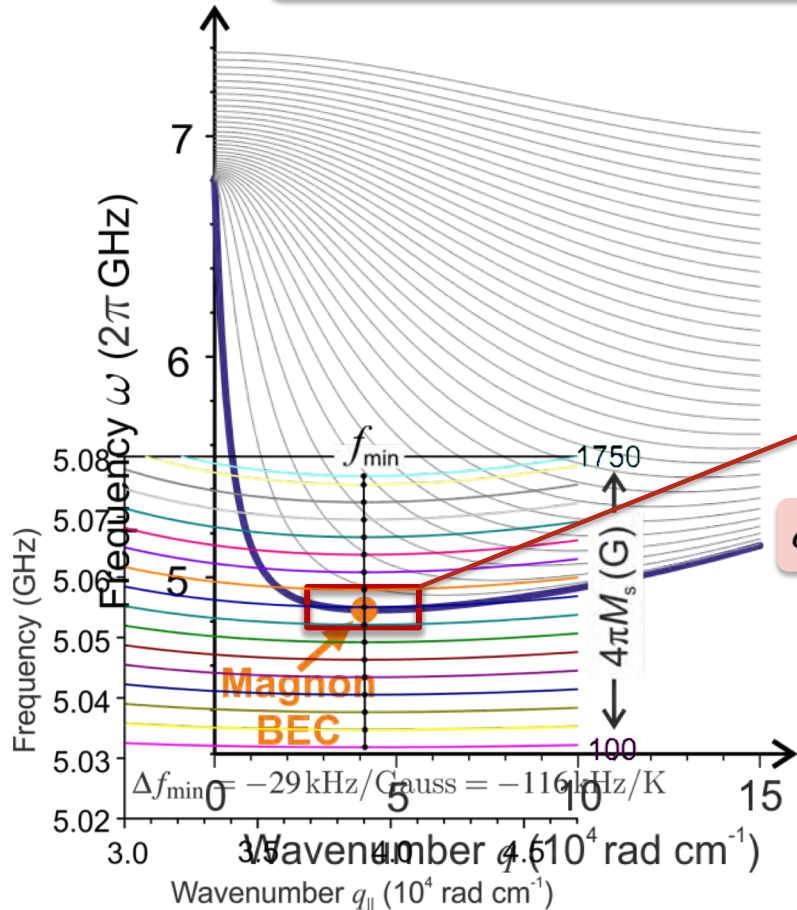
$f_p/2$

Magnon thermalization due to 4-particle scattering:
incoherent magnon gas

Bose-Einstein magnon condensate

Supercurrent in magnon BEC

Supercurrent: Flow of particles due to **phase gradient** of the **condensate's wavefunction**



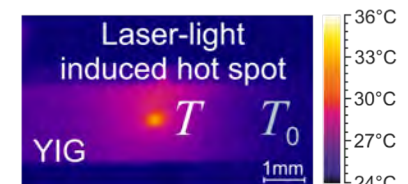
Complex BEC wave function: $\psi(\vec{r}, t)$

BEC density: $N_c = |\psi|^2$

BEC phase: $\varphi = \arg(\psi)$

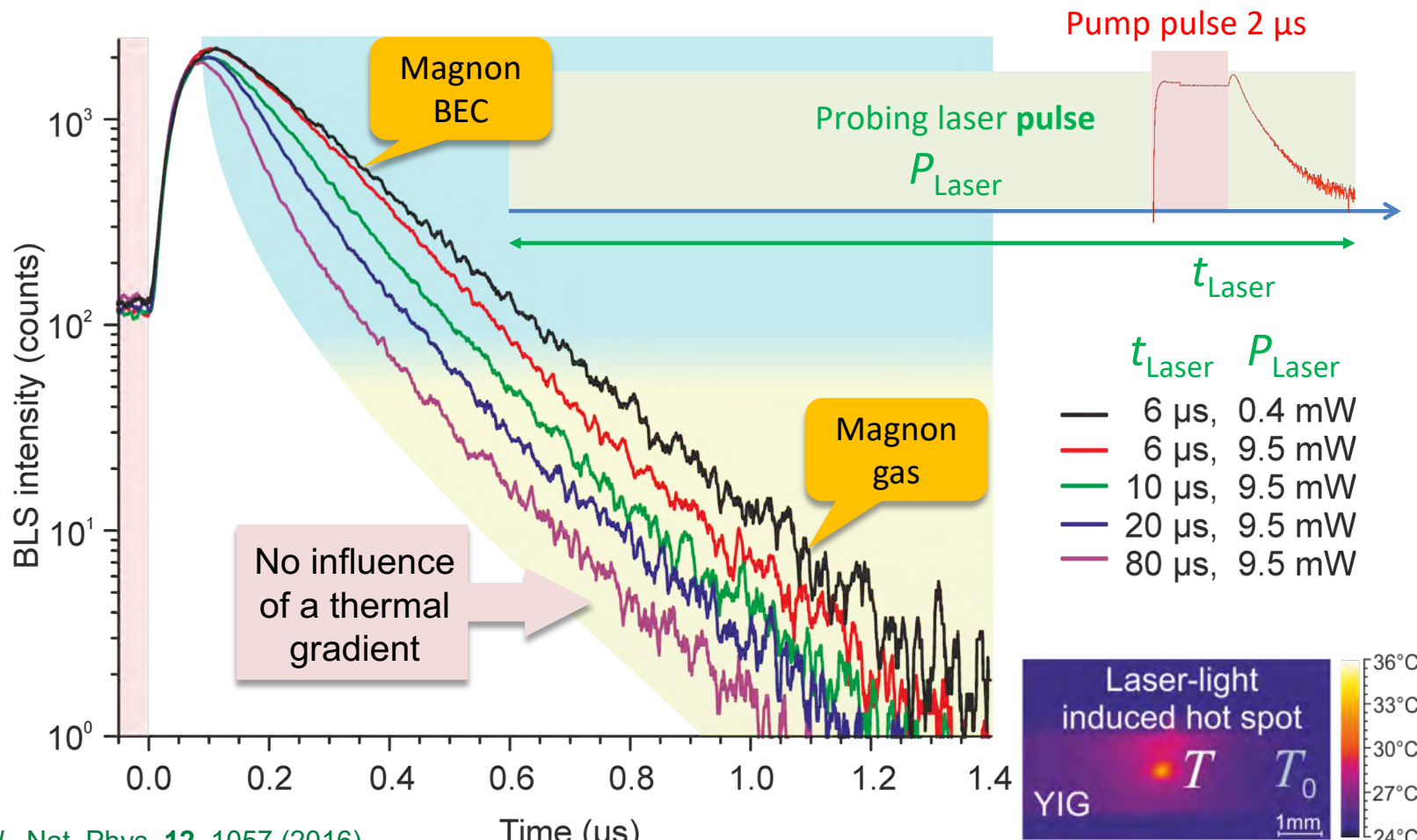
Supercurrent

$$\vec{J}(\vec{r}, t) = \frac{\hbar}{m} N_c \nabla \varphi$$



By changing probing laser **power** or laser pulse **duration** it is possible to control the **phase** of the magnon BEC

Dynamics of condensed magnons in thermal gradient

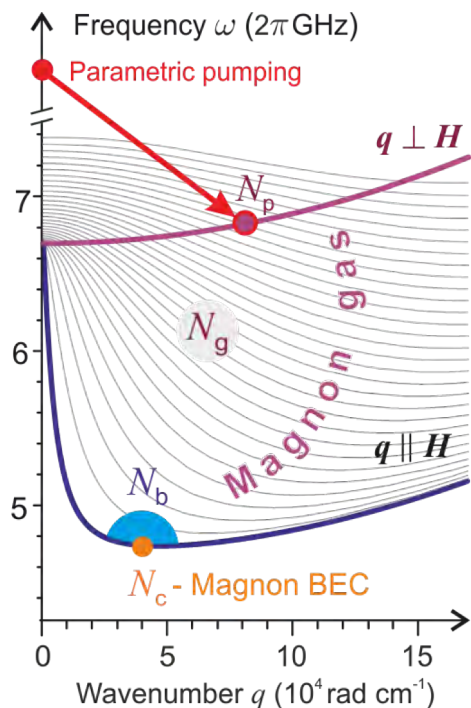


D. A. Bozhko *et al.*, Nat. Phys. **12**, 1057 (2016)

Dynamics of condensed magnons in thermal gradient - theory

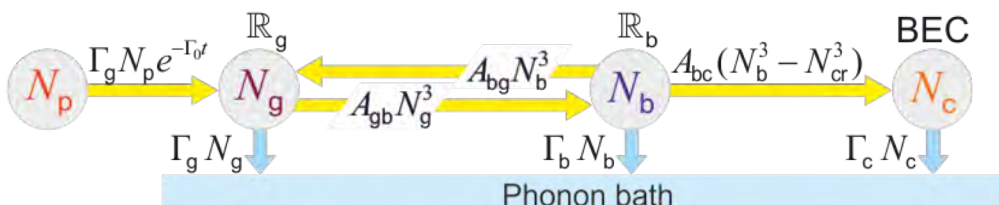
Dynamics of condensed magnons $N_c(t)$, magnons in gaseous states $N_g(t)$ and gaseous magnons at the bottom of SW spectrum $N_b(t)$ described using rate equations

Without thermal gradient \rightarrow



$$\begin{aligned}\frac{\partial N_g}{\partial t} &= -\Gamma_g N_g + \Gamma_g N_p e^{-\Gamma_0 t} - A_{gb} N_g^3 + A_{bg} N_b^3 \\ \frac{\partial N_b}{\partial t} &= -\Gamma_b N_b + A_{gb} N_g^3 - A_{bg} N_b^3 - A_{bc} (N_b^3 - N_{cr}^3) \Theta(N_b - N_{cr}) \\ \frac{\partial N_c}{\partial t} &= -\Gamma_c N_c + A_{bc} (N_b^3 - N_{cr}^3) \Theta(N_b - N_{cr})\end{aligned}$$

N_{cr} – a critical number of magnons at which the chemical potential μ of the magnon gas reaches ω_{min}



D. A. Bozhko *et al.*, Nat. Phys. **12**, 1057 (2016)

Dynamics of condensed magnons in thermal gradient - theory

Dynamics of condensed magnons $N_c(t)$, magnons in gaseous states $N_g(t)$ and gaseous magnons at the bottom of SW spectrum $N_b(t)$ described using rate equations

With thermal gradient 

Supercurrent

$$\vec{J}(\vec{r}, t) = \frac{\hbar}{m} N_c \nabla \varphi \text{ gradient}$$

BEC density: $N_c = |\psi|^2$

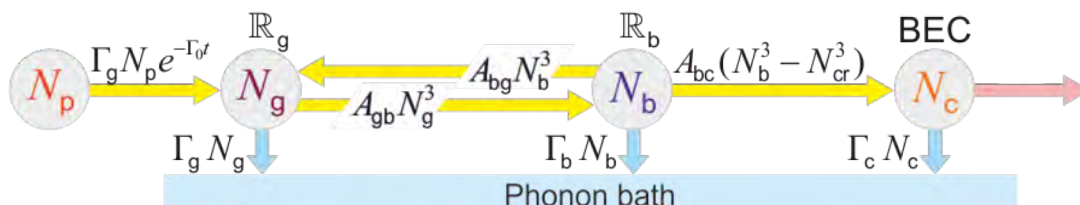
BEC phase: $\varphi = \arg(\psi)$

$$\text{Magnon mass: } m = \hbar / \left(\frac{\partial^2 \omega(q)}{\partial q^2} \right)$$

Complex BEC wave function: $\psi(\vec{r}, t)$

$$\begin{aligned}\frac{\partial N_g}{\partial t} &= -\Gamma_g N_g + \Gamma_g N_p e^{-\Gamma_0 t} - A_{gb} N_g^3 + A_{bg} N_b^3 \\ \frac{\partial N_b}{\partial t} &= -\Gamma_b N_b + A_{gb} N_g^3 - A_{bg} N_b^3 - A_{bc} (N_b^3 - N_{cr}^3) \Theta(N_b - N_{cr}) \\ \frac{\partial N_c}{\partial t} &= -\Gamma_c N_c + A_{bc} (N_b^3 - N_{cr}^3) \Theta(N_b - N_{cr}) - \frac{\partial J(\vec{r}, t)}{\partial \vec{r}}\end{aligned}$$

Additional decrease of population of condensed magnons $N_c(t)$ due to magnon **supercurrent** $\vec{J}(\vec{r}, t)$



D. A. Bozhko *et al.*, Nat. Phys. **12**, 1057 (2016)

Dynamics of condensed magnons in thermal gradient - theory

Dynamics of condensed magnons $N_c(t)$, magnons in gaseous states $N_g(t)$ and gaseous magnons at the bottom of SW spectrum $N_b(t)$ described using rate equations

With thermal gradient 

2D supercurrent

$$J_x = N_c D_x \frac{\partial \phi}{\partial x}$$

$$J_y = N_c D_y \frac{\partial \phi}{\partial y}$$

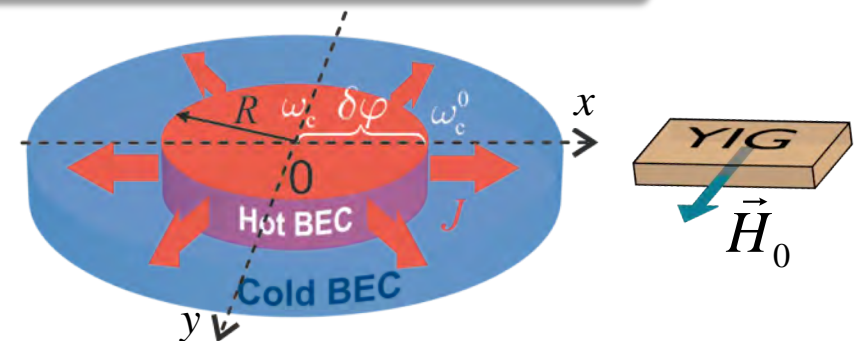
$$\begin{aligned} \frac{\partial N_g}{\partial t} &= -\Gamma_g N_g + \Gamma_g N_p e^{-\Gamma_0 t} - A_{gb} N_g^3 + A_{bg} N_b^3 \\ \frac{\partial N_b}{\partial t} &= -\Gamma_b N_b + A_{gb} N_g^3 - A_{bg} N_b^3 - A_{bc} (N_b^3 - N_{cr}^3) \Theta(N_b - N_{cr}) \\ \frac{\partial N_c}{\partial t} &= -\Gamma_c N_c + A_{bc} (N_b^3 - N_{cr}^3) \Theta(N_b - N_{cr}) - \frac{\partial J_x}{\partial x} - \frac{\partial J_y}{\partial y} \end{aligned}$$

Additional decrease of population of condensed magnons $N_c(t)$ due to magnon **supercurrent** $\vec{J}(x, y, t)$

Anisotropic dispersion coefficients

$$D_x = \frac{1}{2} \frac{\partial^2 \omega(\vec{q})}{\partial q_x^2}$$

$$D_y = \frac{1}{2} \frac{\partial^2 \omega(\vec{q})}{\partial q_y^2}$$



Dynamics of condensed magnons in thermal gradient - theory

Dynamics of condensed magnons $N_c(t)$, magnons in gaseous states $N_g(t)$ and gaseous magnons at the bottom of SW spectrum $N_b(t)$ described using rate equations

With thermal gradient →

2D supercurrent

$$J_x = N_c D_x \frac{\partial \phi}{\partial x}$$

$$J_y = N_c D_y \frac{\partial \phi}{\partial y}$$

$$\begin{aligned}\frac{\partial N_g}{\partial t} &= -\Gamma_g N_g + \Gamma_g N_p e^{-\Gamma_0 t} - A_{gb} N_g^3 + A_{bg} N_b^3 \\ \frac{\partial N_b}{\partial t} &= -\Gamma_b N_b + A_{gb} N_g^3 - A_{bg} N_b^3 - A_{bc} (N_b^3 - N_{cr}^3) \Theta(N_b - N_{cr}) \\ \frac{\partial N_c}{\partial t} &= -\Gamma_c N_c + A_{bc} (N_b^3 - N_{cr}^3) \Theta(N_b - N_{cr}) - \frac{\partial J_x}{\partial x} - \frac{\partial J_y}{\partial y}\end{aligned}$$

Additional decrease of population of condensed magnons $N_c(t)$ due to magnon **supercurrent** $\vec{J}(x, y, t)$

Anisotropic dispersion coefficients

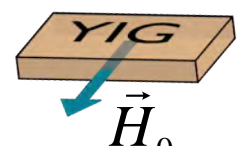
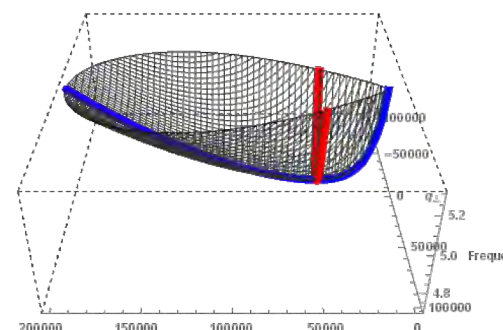
$$D_x = \frac{1}{2} \frac{\partial^2 \omega(\vec{q})}{\partial q_x^2}$$

$$D_y = \frac{1}{2} \frac{\partial^2 \omega(\vec{q})}{\partial q_y^2}$$

In experiment:

$$D_x \approx 21 D_y$$

$$J_T = J_x \gg J_y$$



Dynamics of condensed magnons in thermal gradient - theory

Dynamics of condensed magnons $N_c(t)$, magnons in gaseous states $N_g(t)$ and gaseous magnons at the bottom of SW spectrum $N_b(t)$ described using rate equations

With thermal gradient \rightarrow

1D thermally driven supercurrent

$$J_T = N_c D_x \frac{\partial \varphi}{\partial x}$$

$$\delta\varphi = \delta\omega_c(x) t$$

a weak frequency shift
of the BEC wave function
due to temperature change

$$\frac{\partial N_g}{\partial t} = -\Gamma_g N_g + \Gamma_g N_p e^{-\Gamma_0 t} - A_{gb} N_g^3 + A_{bg} N_b^3$$

$$\frac{\partial N_b}{\partial t} = -\Gamma_b N_b + A_{gb} N_g^3 - A_{bg} N_b^3 - A_{bc} (N_b^3 - N_{cr}^3) \Theta(N_b - N_{cr})$$

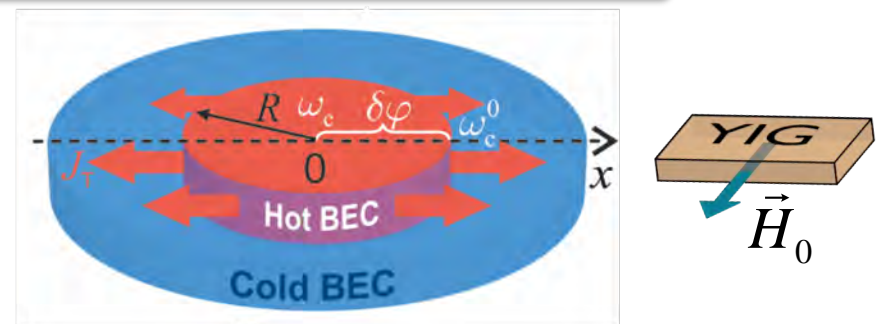
$$\frac{\partial N_c}{\partial t} = -\Gamma_c N_c + A_{bc} (N_b^3 - N_{cr}^3) \Theta(N_b - N_{cr}) - \frac{\partial J_T}{\partial x}$$

Additional decrease of population of condensed magnons $N_c(t)$ due to magnon **supercurrent** $J_T(x,t)$

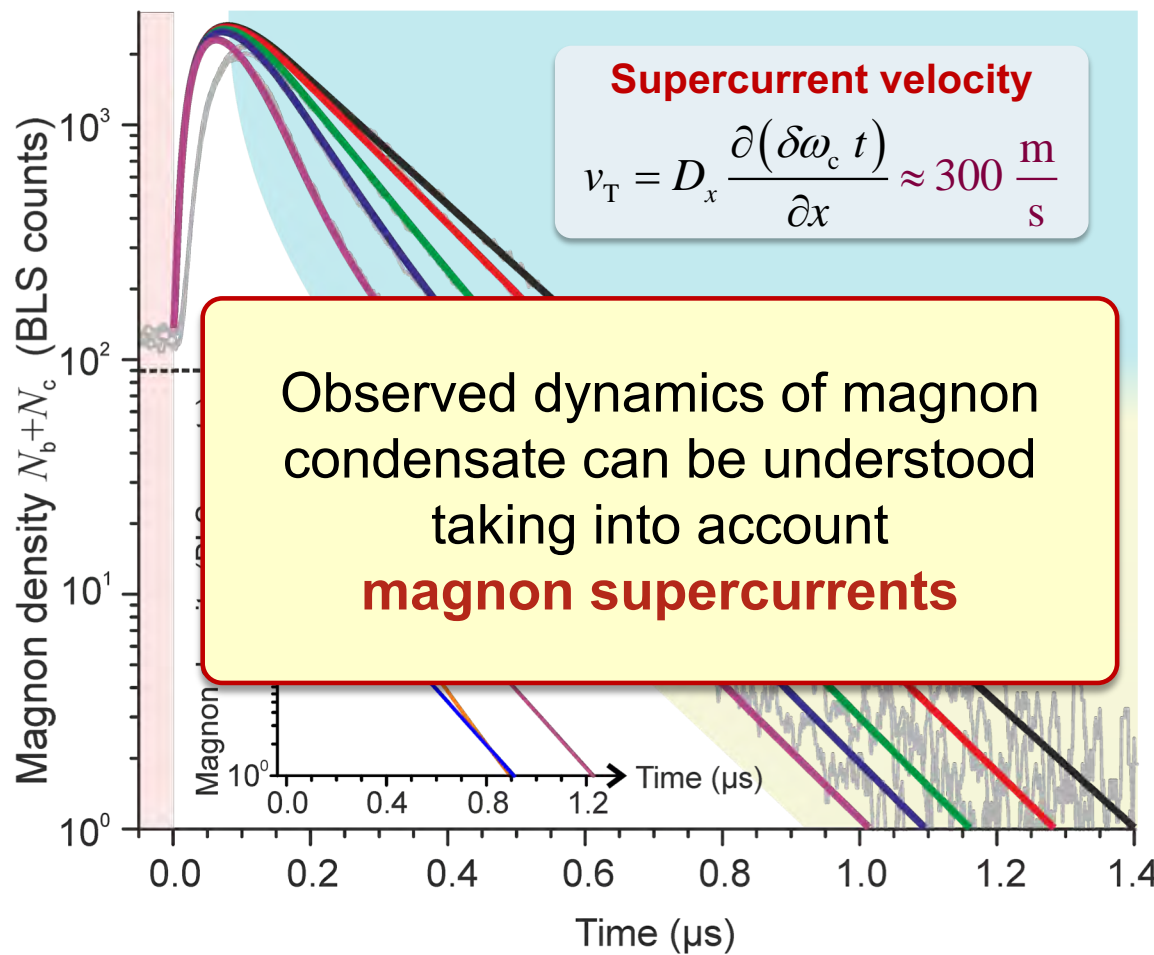
In experiment:

$$D_x \approx 21 D_y$$

$$J_T = J_x \gg J_y$$



Dynamics of condensed magnons in thermal gradient - comparison with theory



$$\delta\varphi = \delta\omega_c(T)t$$

Thermally induced frequency shift of the magnon BEC

$$\delta\omega_c(T) / 2\pi$$

- 0 kHz
- 25 kHz
- 100 kHz
- 198 kHz
- 550 kHz

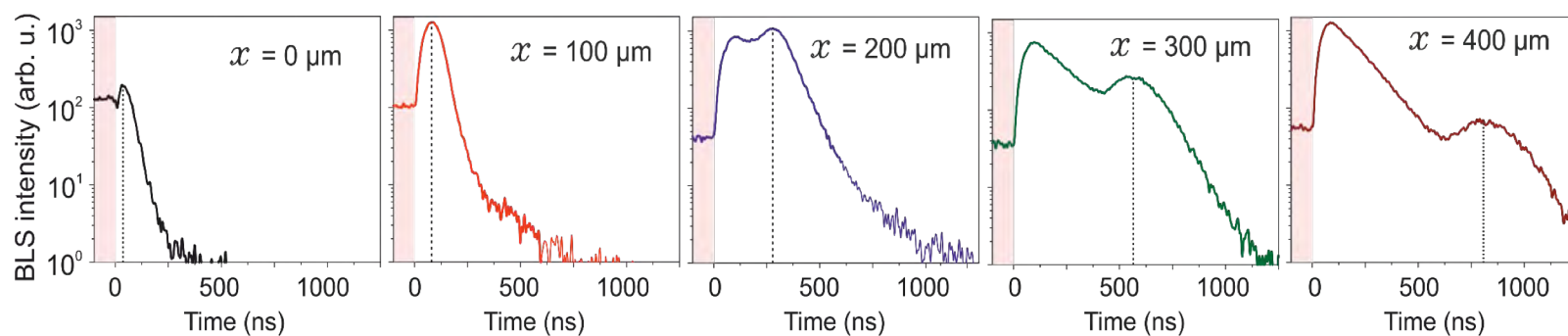
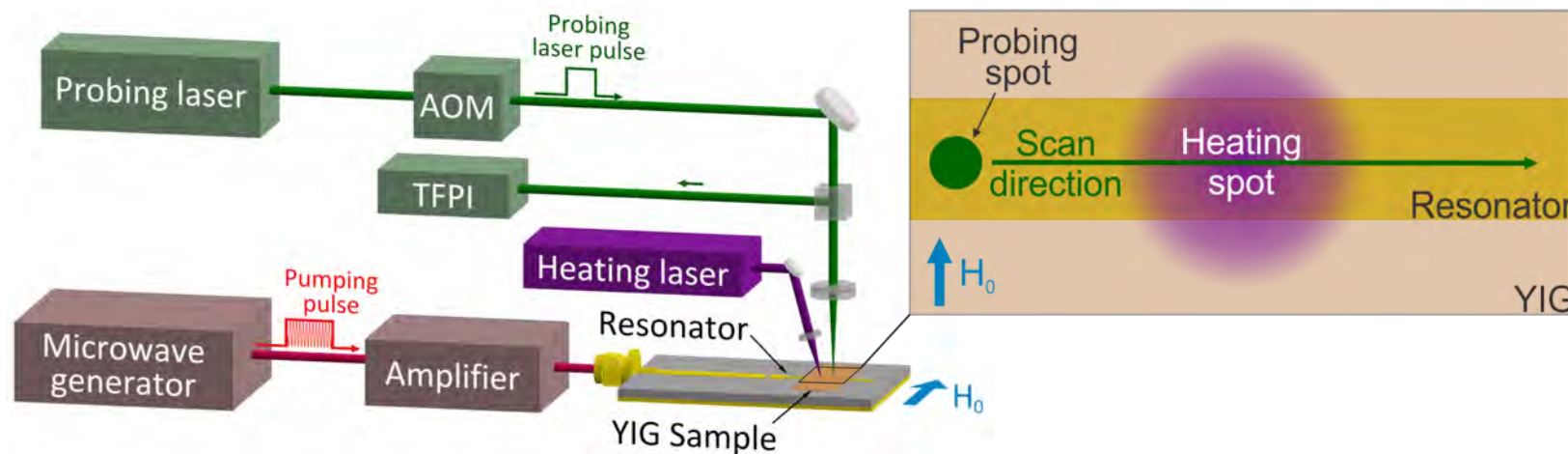


Corresponding maximal temperature change

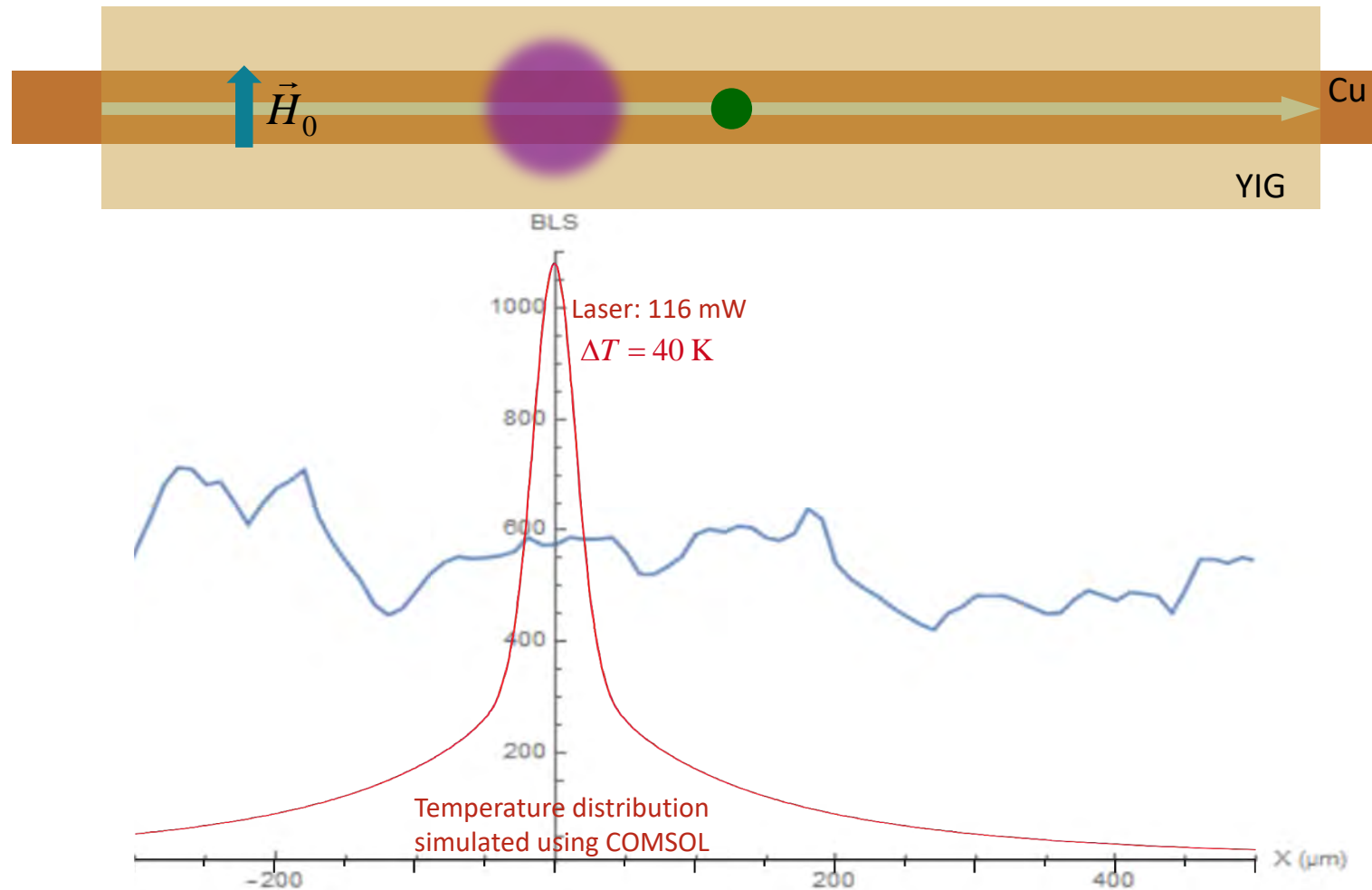
$$4.7 \text{ K}$$

D. A. Bozhko *et al.*, Nat. Phys. **12**, 1057 (2016)

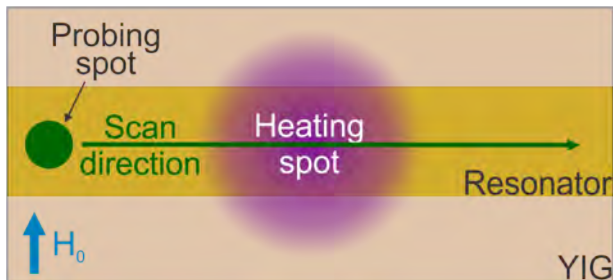
Non-local measurement: Supercurrent magnon transport



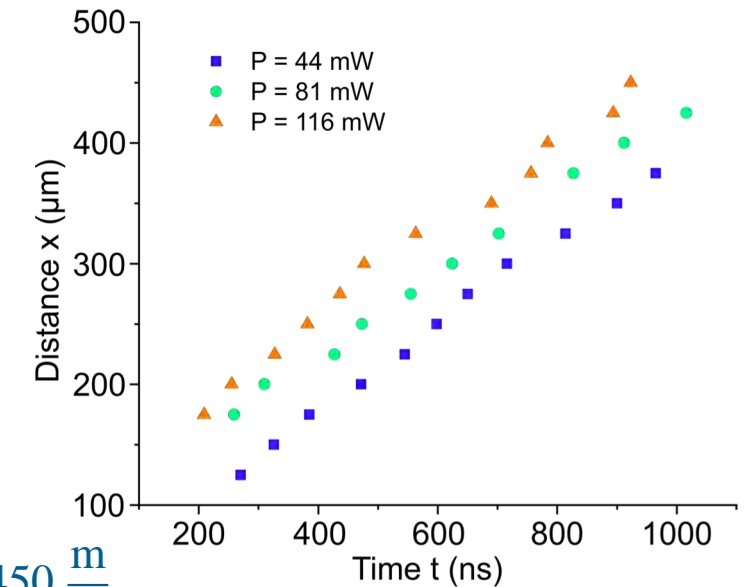
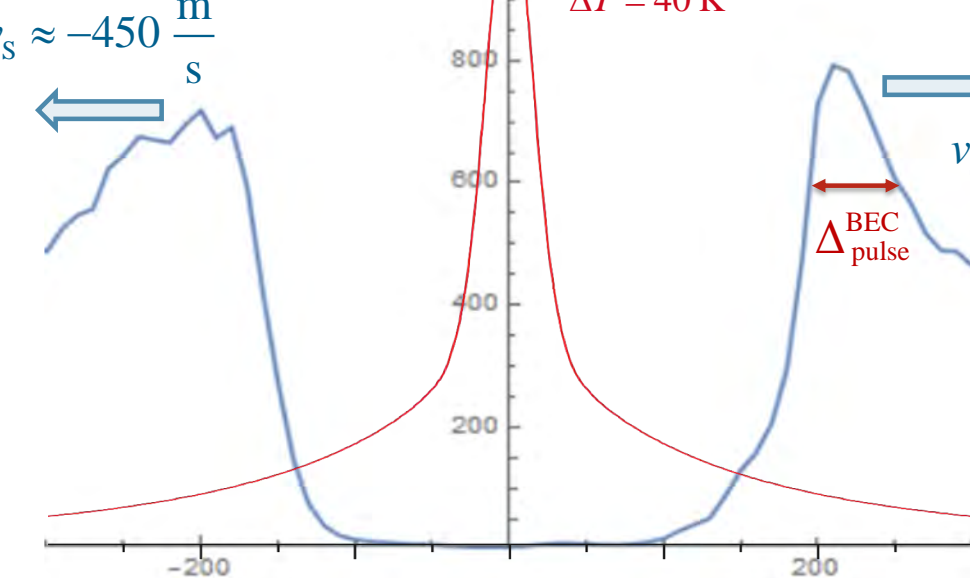
Non-local measurement: Supercurrent magnon transport



Non-local measurement: Supercurrent magnon transport



$$v_s \approx -450 \frac{\text{m}}{\text{s}}$$



Non-local measurement: Second magnonic sound scenario

Gross-Pitaevskii equation for dynamic behavior of the magnon BEC

$$\left[i \frac{\partial}{\partial t} + D_x \frac{\partial^2}{\partial x^2} - W |\psi|^2 \right] \psi = 0$$

Dispersion coefficient

$$D_x = \frac{1}{2} \frac{\partial^2 \omega(\vec{q})}{\partial q_x^2}$$

Amplitude of four-wave **repulsive** interaction

$$W > 0$$

O. Dzyapko *et al.*, Phys. Rev. B **96**, 064438 (2017)

Stationary solution: $\psi(x,t) = \sqrt{N_c} \exp(-iWN_c t)$

Magnon BEC density

$$N_c$$

Bogoliubov dispersion law for small perturbations on the background of the stationary solution
(second sound)

$$\omega(q) = c_s q \sqrt{1 + D_x q^2 / 2WN_c}$$

$$D_x q^2 \ll 2WN_c$$

$$\omega(q) = c_s q$$

second sound velocity

$$c_s = \sqrt{2D_x WN_c}$$

$$D_x q^2 \gg 2WN_c$$

$$\omega(q) = D_x q^2$$

Estimations for $c_s = v_s \approx 450$ m/s and $D_x \approx 7.45$ cm²/s

Nonlinear frequency shift: $2WN_c \approx 2\pi \cdot 44$ MHz

For 116 mW laser power the BEC pulse width $\Delta_{\text{pulse}}^{\text{BEC}} \approx 44$ μm
 $q = \pi / \Delta_{\text{pulse}}^{\text{BEC}} \approx 720$ rad/cm $D_x q^2 \approx 2\pi \cdot 0.52$ MHz

Non-local measurement: Second magnonic sound scenario

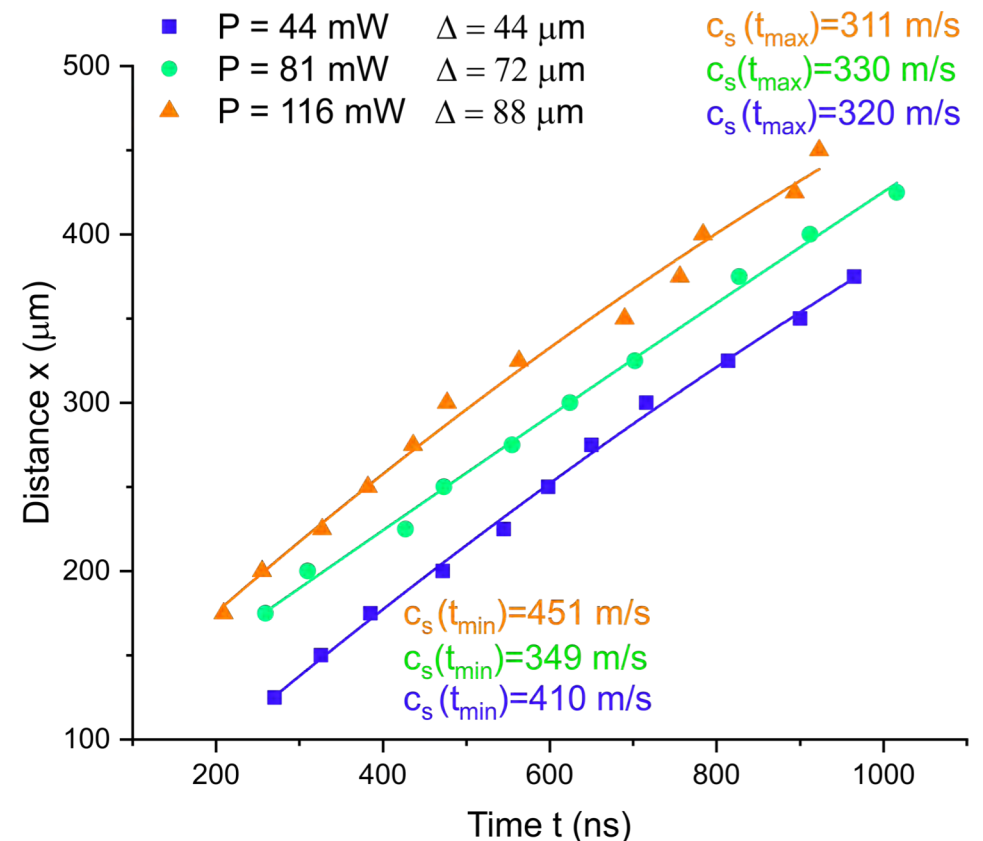
$$\omega(q) = c_s q, \quad c_s = \sqrt{2D_x W N_c}$$

- The sound velocity c_s must be **independent** on the excitation conditions i.e. the heating laser power, which determine the BEC pulse width $\Delta_{\text{pulse}}^{\text{BEC}}$

100% change in $\Delta_{\text{pulse}}^{\text{BEC}}$  9% change in c_s

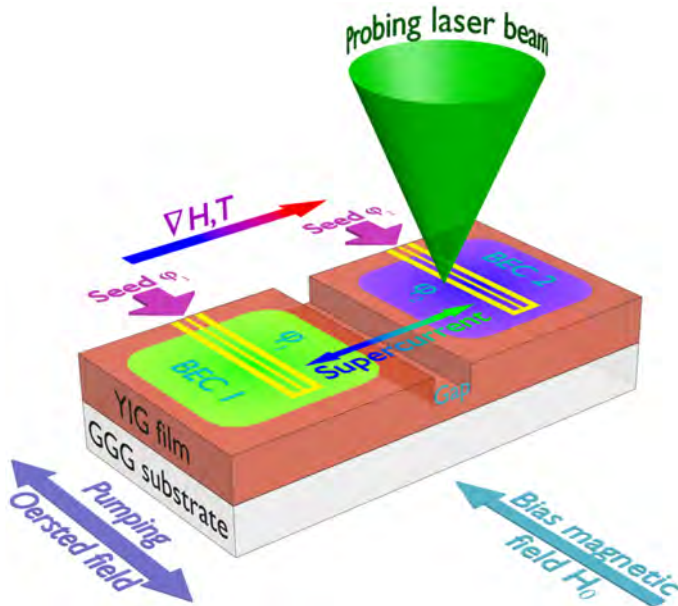
- During the pulse propagation, the amplitude of the background condensate decays and the sound velocity also has to decay

The sound velocity decrease is clear visible from parabolic fits !



Both statements are well satisfied

Outlook 1: AC/DC magnon Josephson effect



1. Use of magnon supercurrent for applications

Magnon supercurrent between two spatially separated condensates

- Phase difference is realized using initial seeding of each condensate
- Coupling strength of BECs can be varied by changing the size of the gap between the condensates
- Additional gradients of magnetic field or temperature can be applied to induce time-dependent phase shift

Modified complex Ginzburg-Landau equation

| | | | | |
|---|----------------------|---------------------------------|-------------------|----------------|
| Phase accumulation from external potential | Condensate motion | Nonlinear phase accumulation | Magnon damping | BEC seeding |
|---|----------------------|---------------------------------|-------------------|----------------|

$$i\hbar \frac{\partial \psi}{\partial t} = \left(\hbar \omega_0(x, T, H) - \frac{\hbar^2}{2m} \nabla^2 + \hbar N |\psi|^2 \right) \psi + i\hbar(\eta - \beta |\psi|^2) \psi + if(\mathbf{r}, t)$$

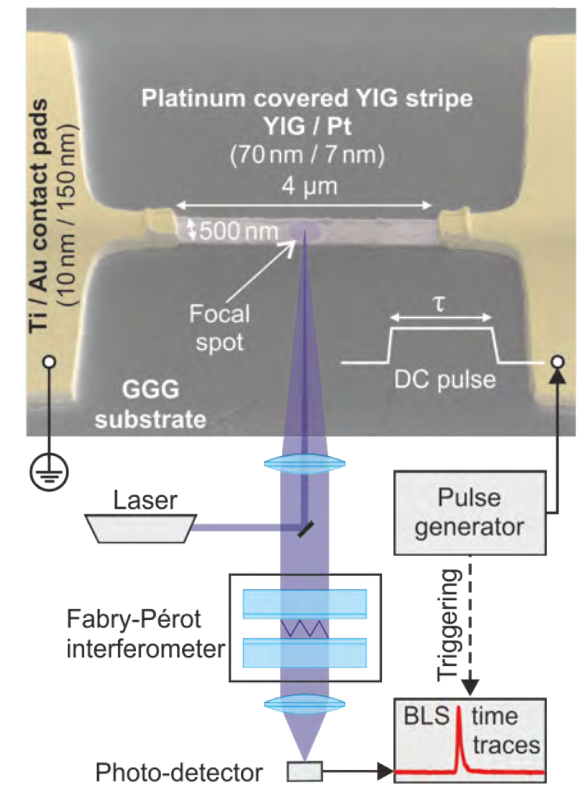
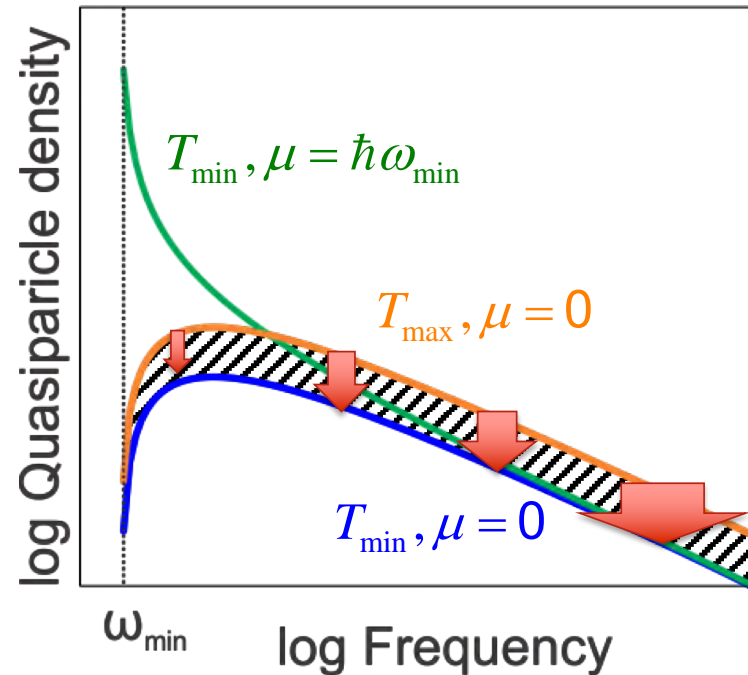
Outlook 2: Microwave-free creation of a magnon BEC

2. Are there other ways how to create a magnon BEC state in YIG?

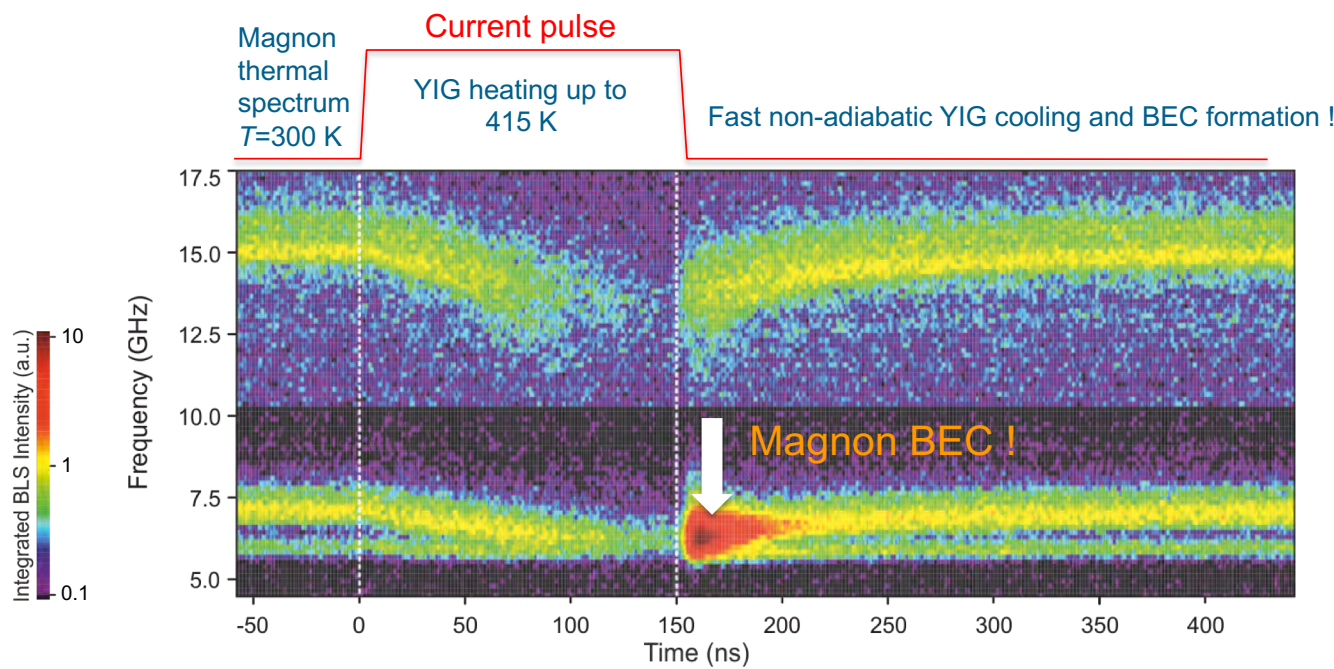
- Yes, by rapid cooling of a magnon-carrying specimen

Bose-Einstein distribution

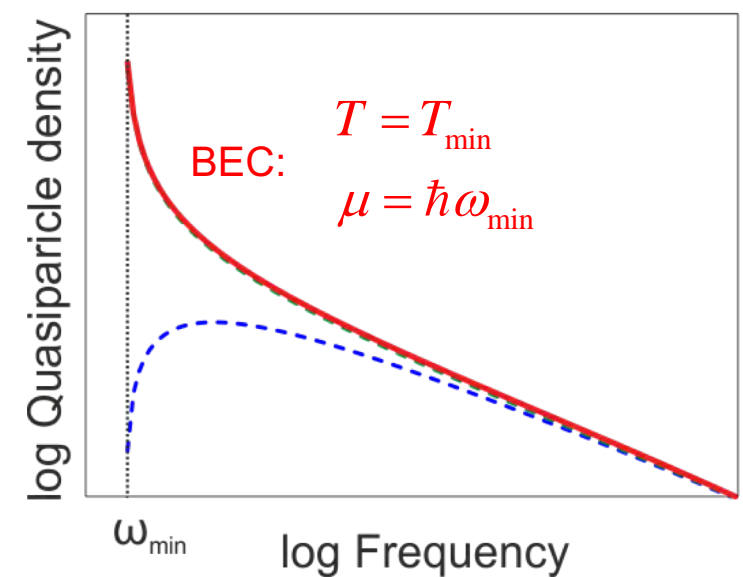
$$\rho(\omega) = \frac{D(\omega)}{\exp\left(\frac{\hbar\omega - \mu}{k_B T}\right) - 1}$$



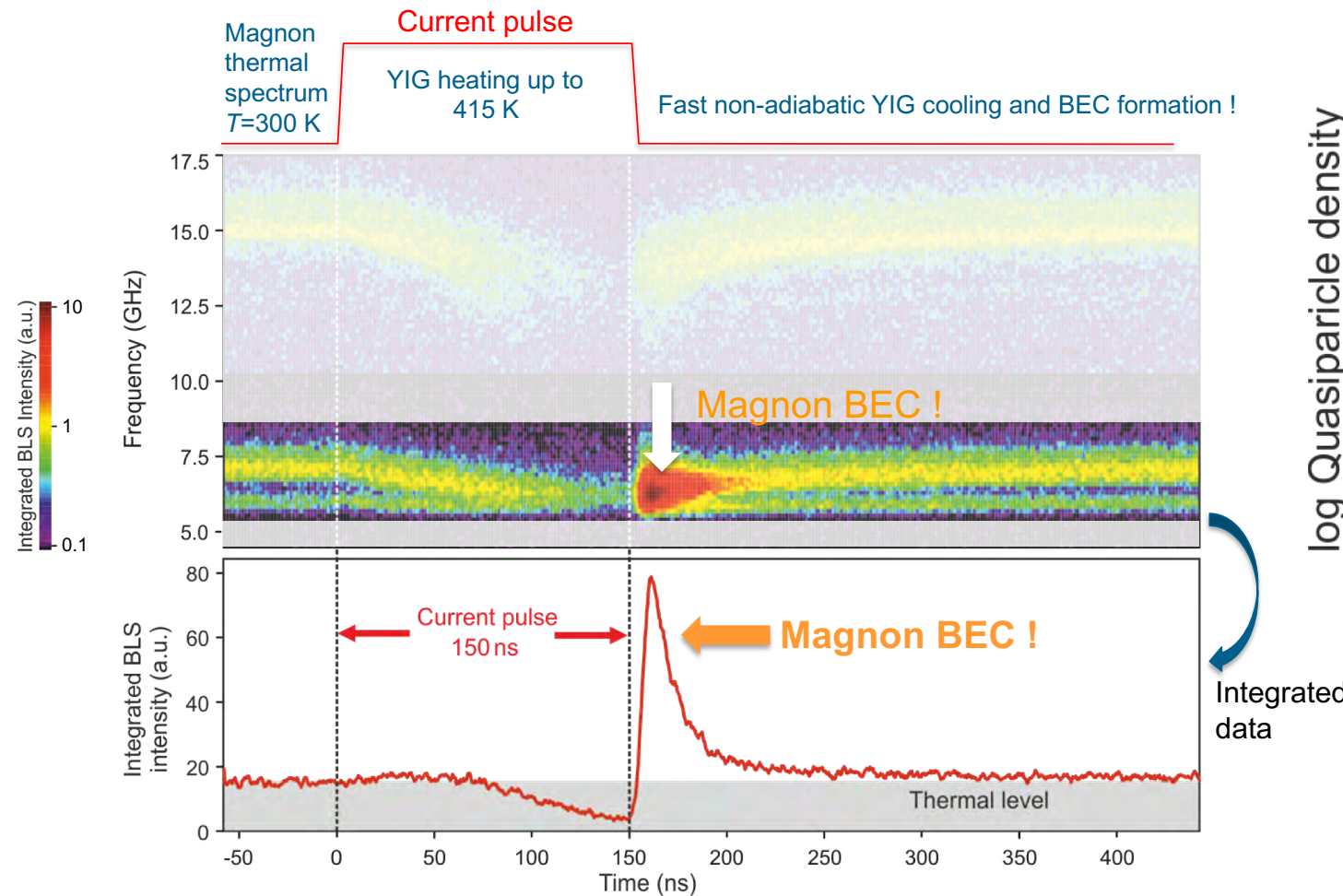
BEC in rapidly cooled magnon gas



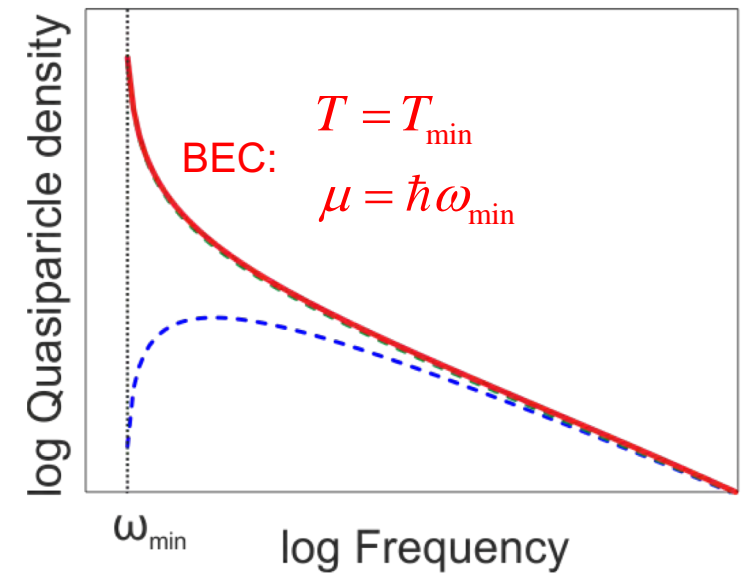
Magnon population distribution



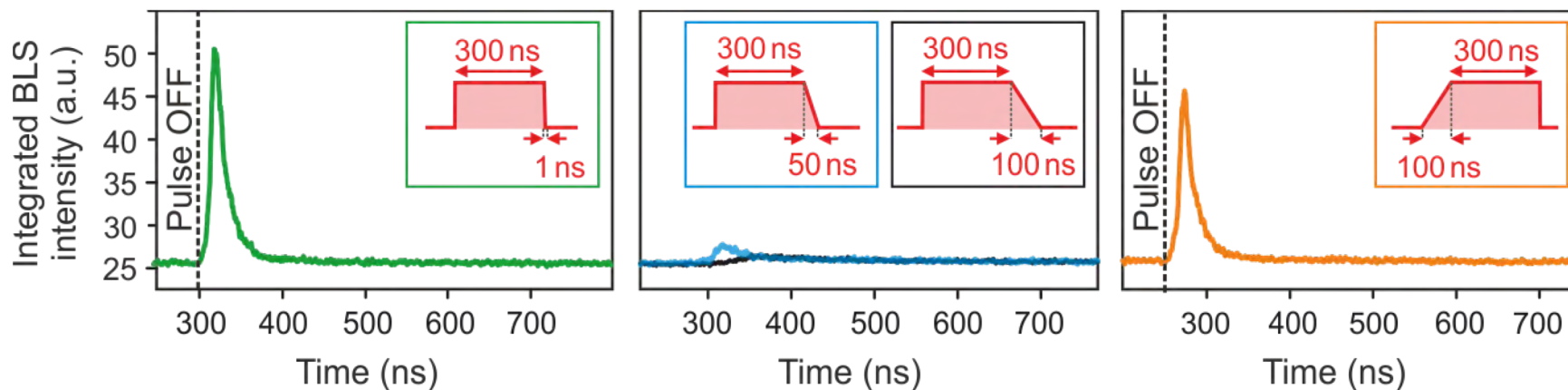
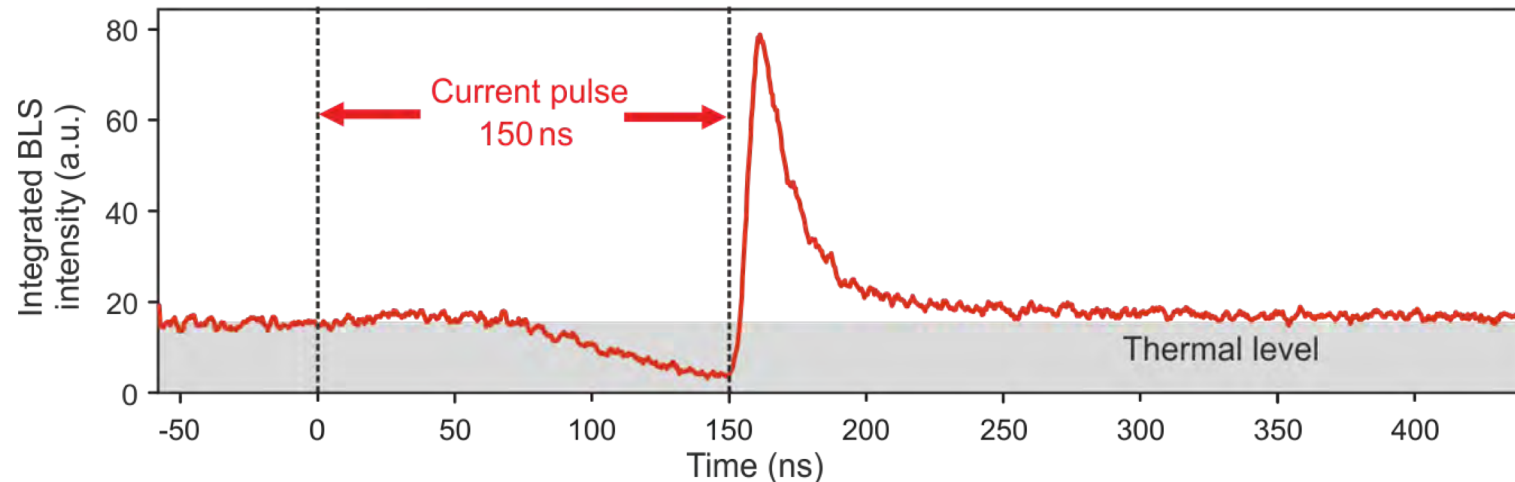
BEC in rapidly cooled magnon gas



Magnon population distribution

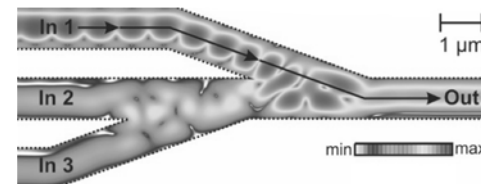


Magnon BEC intensity and cooling rate

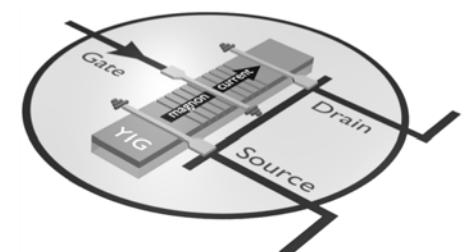


Advanced magnonics

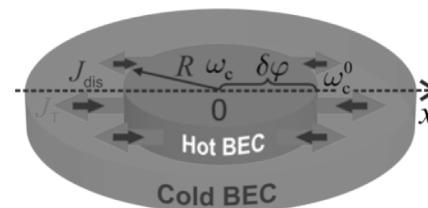
I. Magnon interference logic



II. Non-linear magnonics: Magnon transistor



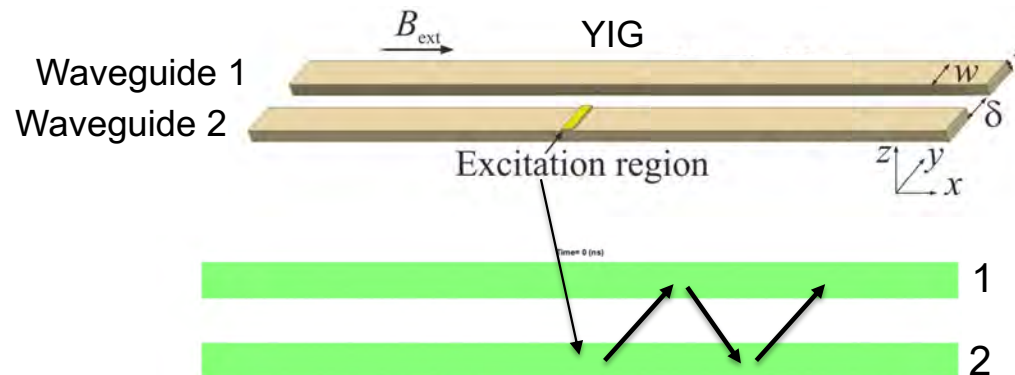
III. Magnonic macroscopic quantum state



IV. Quantum-classical analogies in magnonics

Coupled waveguides

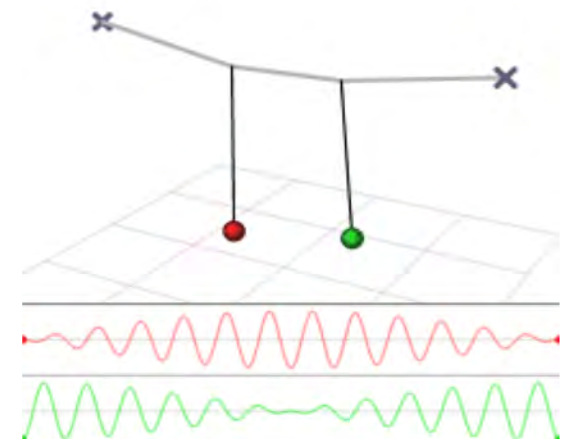
Micromagnetic simulation:



Yttrium Iron Garnet (YIG):

$$\begin{array}{ll} M_s = 1.4 \times 10^5 \text{ A/m} & t = 50 \text{ nm} \\ A = 3.5 \text{ pJ} & w = 100 \text{ nm} \\ \alpha = 2 \times 10^{-4} & \delta = 100 \text{ nm} \end{array}$$

Coupled oscillators

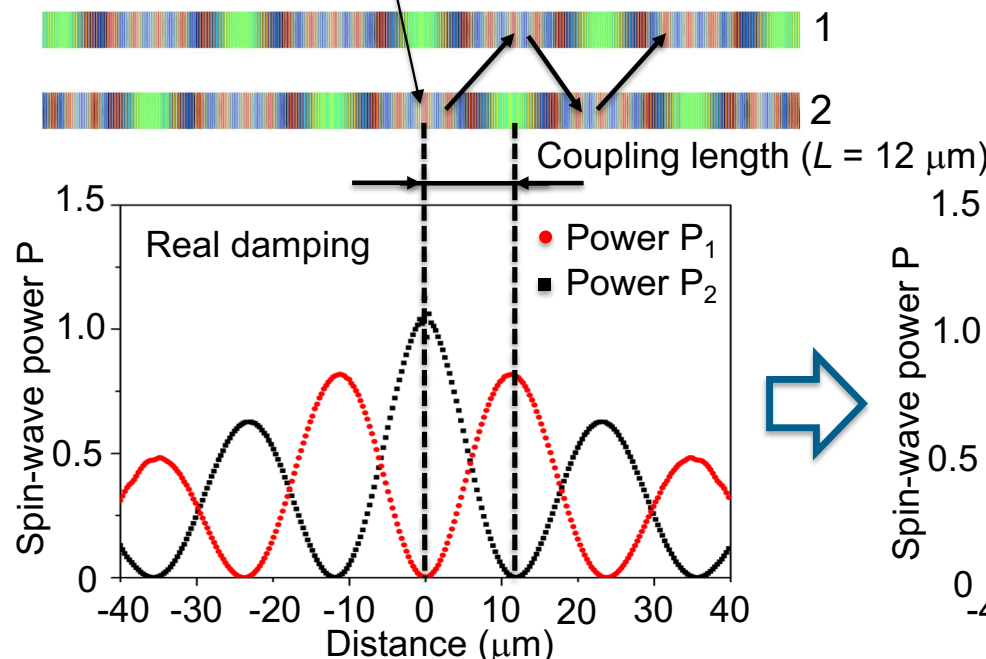
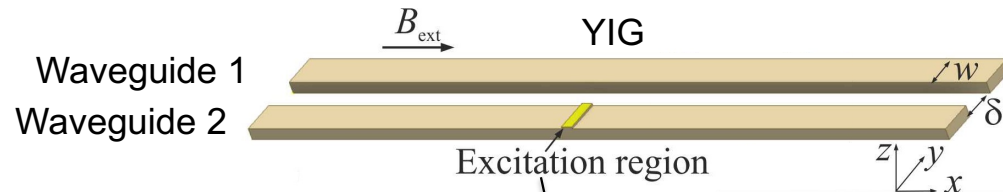


Simulation package Mumax3: A. Vansteenkiste, et al., *AIP Advance* **4**, 107113 (2014)

Source: Wikipedia

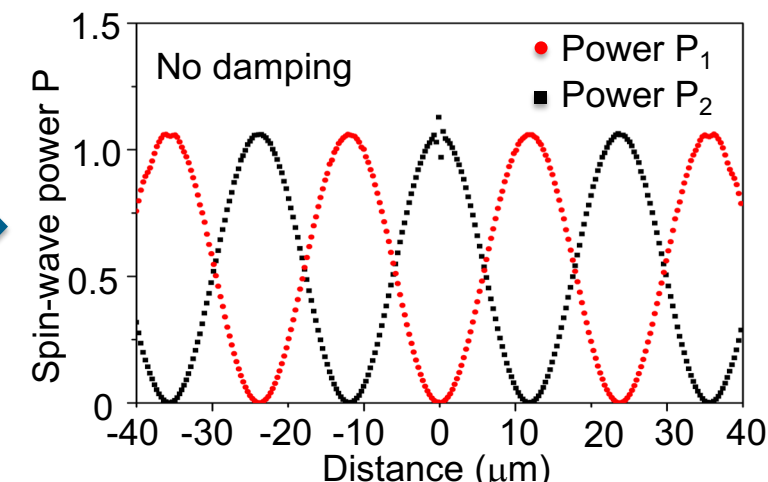
Coupled waveguides

Micromagnetic simulation:



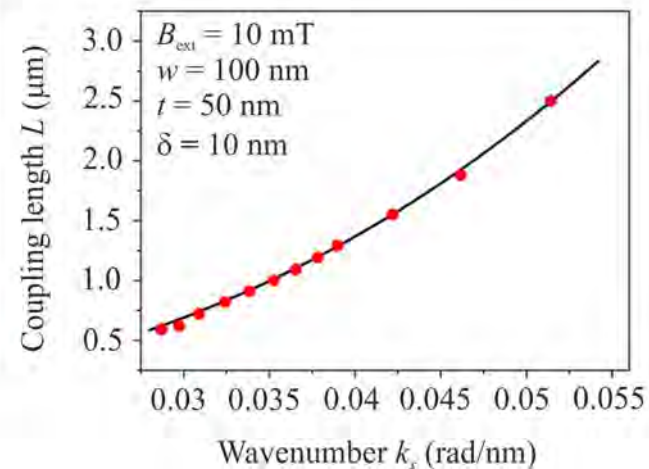
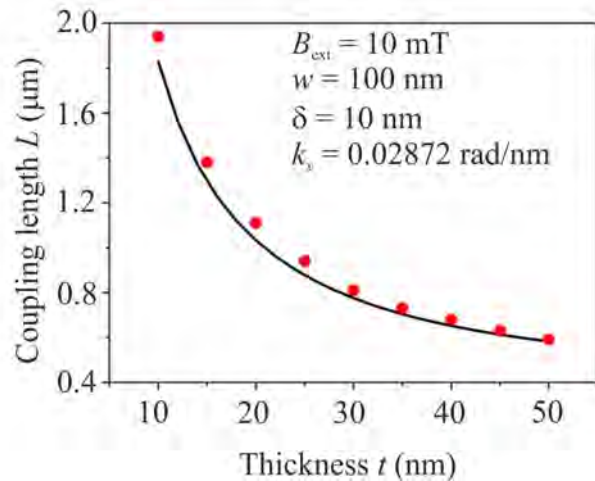
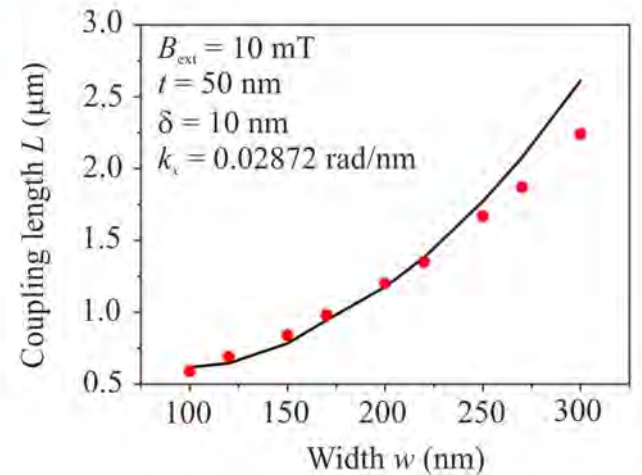
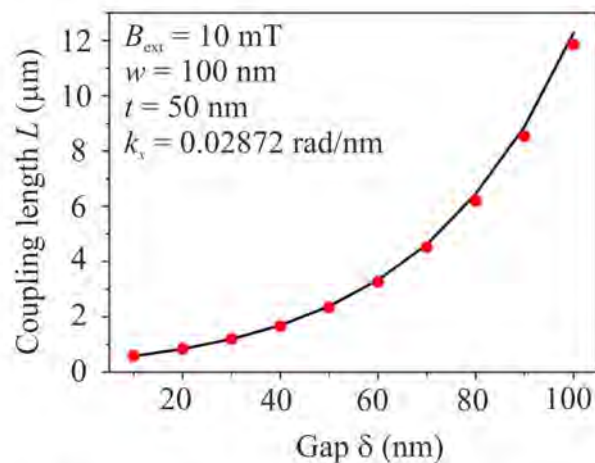
Yttrium Iron Garnet (YIG):

$$\begin{array}{ll} M_s = 1.4 \times 10^5 \text{ A/m} & t = 50 \text{ nm} \\ A = 3.5 \text{ pJ} & w = 100 \text{ nm} \\ \alpha = 2 \times 10^{-4} & \delta = 100 \text{ nm} \end{array}$$

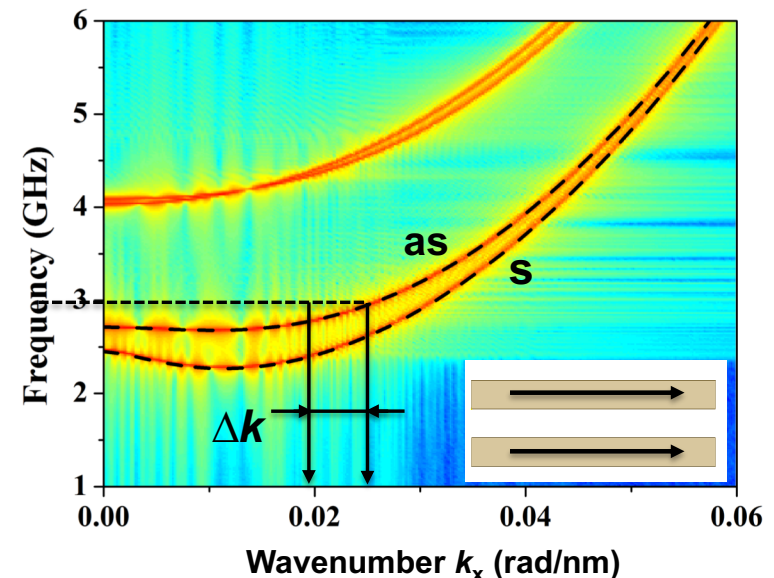
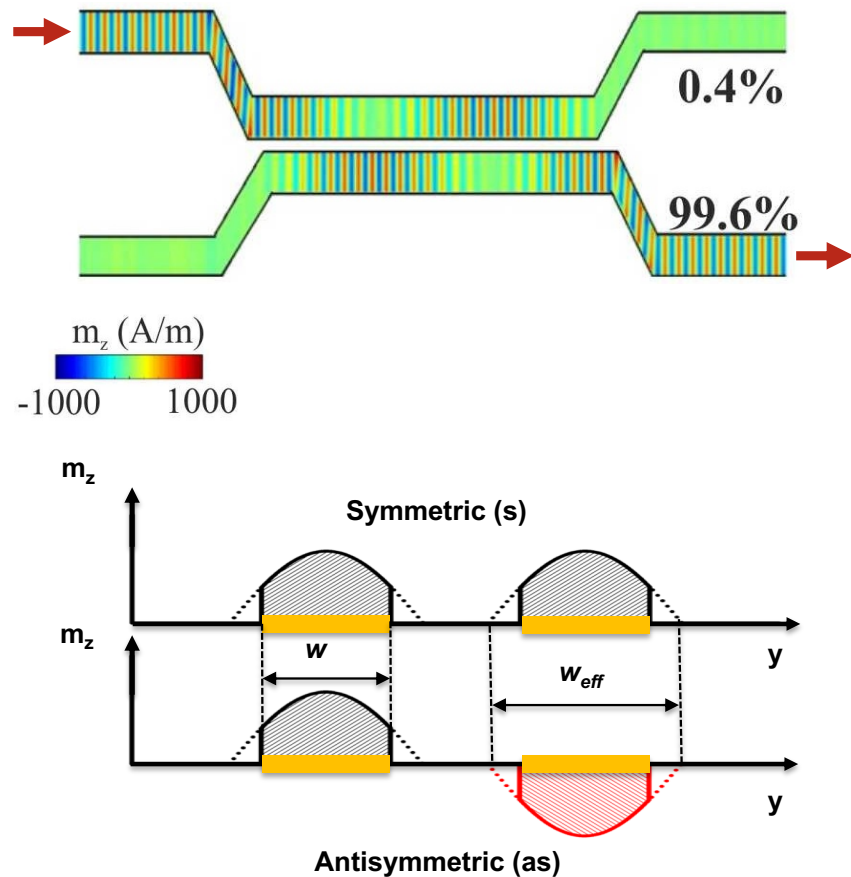


Simulation package Mumax3: A. Vansteenkiste, et al., AIP Advance **4**, 107113 (2014)

Coupling length as a function of system parameters



Magnon directional coupler

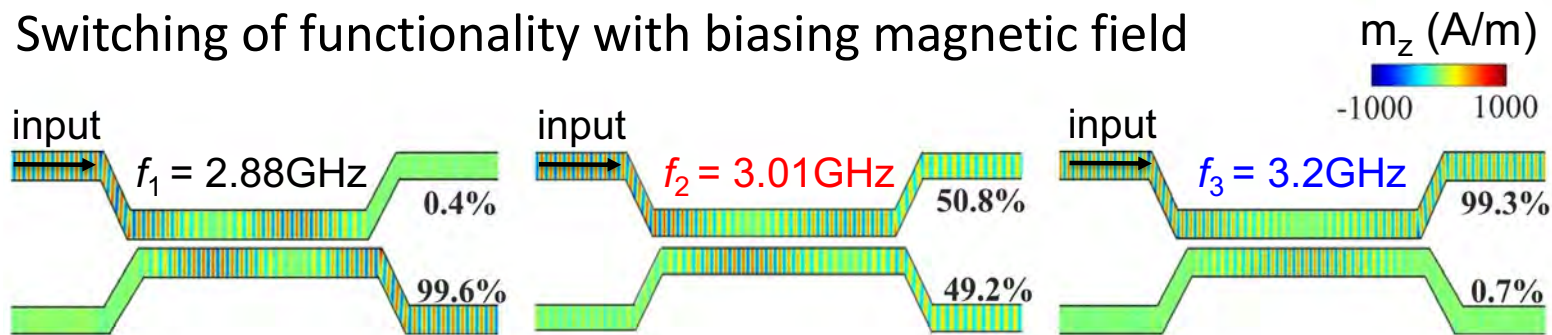


Coupling length:
$$L = \frac{\pi}{\Delta k}$$

Coupling strength:
$$\kappa = \frac{1}{L}$$

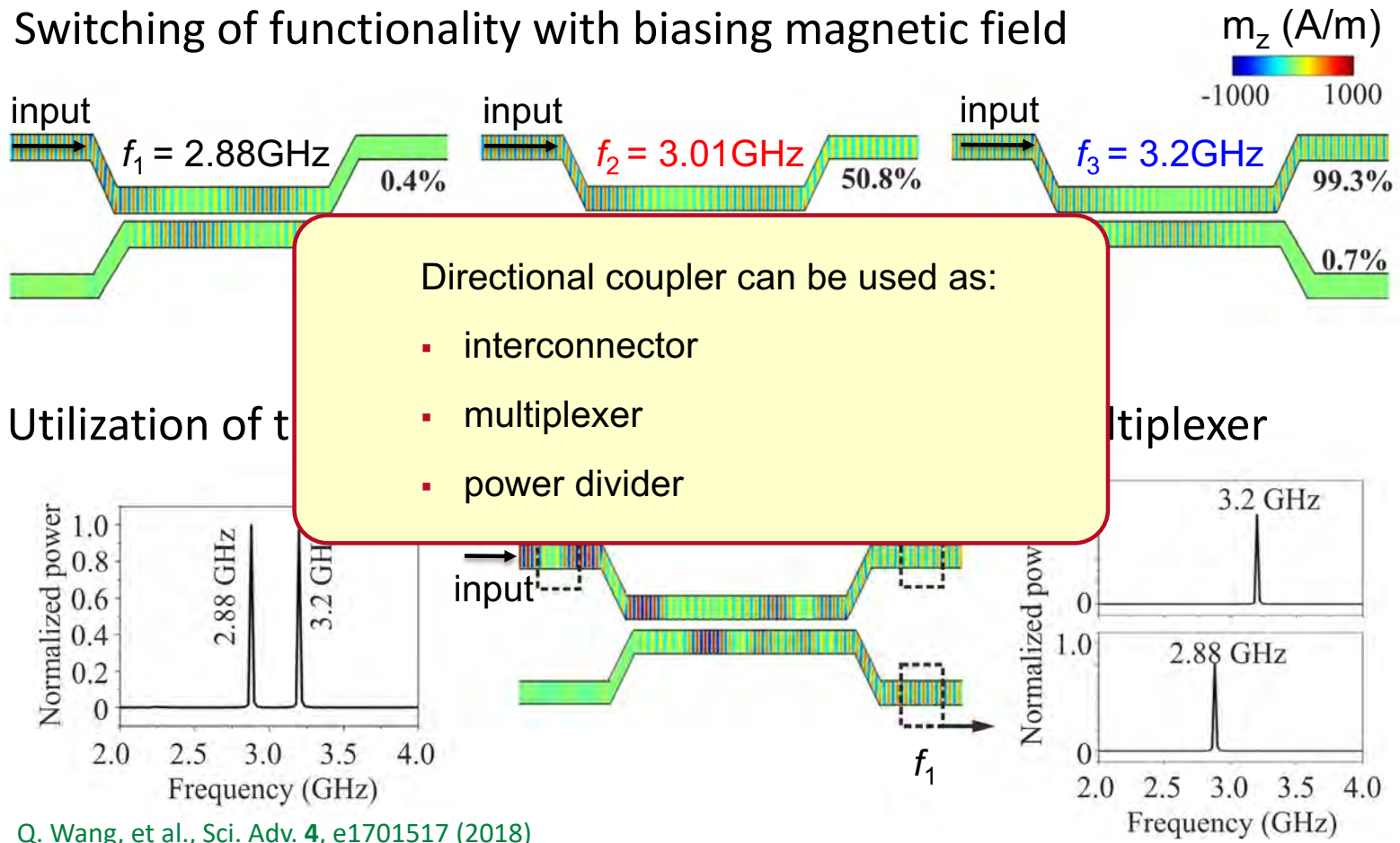
Q. Wang, et al., Sci. Adv. 4, e1701517 (2018)

Functionalities of directional coupler



Q. Wang, et al., Sci. Adv. **4**, e1701517 (2018)

Functionalities of directional coupler



Summary

- Magnon interference logic allows for data processing fully in the magnonic system
- Magnon transistor is an important nonlinear building block of magnonics for future wave-based technology
- Magnon Bose-Einstein condensate (BEC) with zero group velocity can be used for coherent spin transport
- First experimental evidence of creation of a magnon BEC by rapid cooling of a micro-scale YIG/Pt structure
- A magnonic quantum-classical analogy device has been demonstrated (magnonic STIRAP process)

